



HAL
open science

Paleogeographic and structural evolution of northwestern Africa and its Atlantic margins since the early Mesozoic

Jing Ye, Dominique Chardon, Delphine Rouby, François Guillocheau,
Massimo Dall'Asta, Jean-Noel Ferry, Olivier Broucke

► To cite this version:

Jing Ye, Dominique Chardon, Delphine Rouby, François Guillocheau, Massimo Dall'Asta, et al.. Paleogeographic and structural evolution of northwestern Africa and its Atlantic margins since the early Mesozoic. *Geosphere*, 2017, 13 (4), pp.1254-1284. 10.1130/GES01426.1 . insu-01533455

HAL Id: insu-01533455

<https://insu.hal.science/insu-01533455v1>

Submitted on 6 Jun 2017

HAL is a multi-disciplinary open access archive for the deposit and dissemination of scientific research documents, whether they are published or not. The documents may come from teaching and research institutions in France or abroad, or from public or private research centers.

L'archive ouverte pluridisciplinaire **HAL**, est destinée au dépôt et à la diffusion de documents scientifiques de niveau recherche, publiés ou non, émanant des établissements d'enseignement et de recherche français ou étrangers, des laboratoires publics ou privés.



This paper is published under the terms of the CC-BY license.

© 2017 The Authors

Paleogeographic and structural evolution of northwestern Africa and its Atlantic margins since the early Mesozoic

Jing Ye^{1,2}, Dominique Chardon^{1,3}, Delphine Rouby¹, François Guillocheau⁴, Massimo Dall'asta², Jean-Noel Ferry², and Olivier Broucke⁵

¹Géosciences Environnement Toulouse, Université de Toulouse, CNRS, IRD, UPS, CNES, F-31400, France

²TOTAL R&D, Frontier Exploration, Centre Scientifique et Technique Jean Féger (CSTJF), Avenue Larribau, F-64018 Pau Cedex, France

³Institut de recherche pour le développement (IRD) & Département des Sciences de la Terre, Université Ouaga I Professeur Joseph Ki-Zerbo, 01 BP 182, Ouagadougou 01, Burkina Faso

⁴Géosciences-Rennes, UMR 6118, Université de Rennes 1, CNRS, F-35042 Rennes CEDEX, France

⁵TOTAL E&P, Middle East and North Africa—Technical Excellence, La Défense, F-92078 Paris, France

ABSTRACT

The geological evolution of northwestern Africa and its continental margins is investigated in the light of nine Meso-Cenozoic paleogeological maps, which integrate original minimal extent of sedimentary deposits beyond their present-day erosional limits. Mapping is based on a compilation of published original data on the stratigraphy and depositional environments of sediments, structures, magmatism, and low-temperature thermochemistry, as well as on the interpretation of industrial seismic and borehole data.

We show that rifting of the equatorial domain propagated eastward from the Central Atlantic between the Valanginian (ca. 140 Ma) and the Aptian (ca. 112 Ma) as an en echelon strike-slip and rift system connected to an inland rift network. This network defines a six-microplate synrift kinematic model for the African continental domain. We document persistent, long-wavelength eroding marginal upwarps that supplied clastic sediments to the offshore margin basins and a large intracratonic basin. The latter acted as a transient sediment reservoir because the products of its erosion were transferred both to the Tethys (to the north) and the Atlantic Ocean. This paired marginal upwarp-intracratonic basin source-to-sink system was perturbed by the growth of the late Paleogene Hoggar hotspot swell that fragmented the intracratonic basins into five residual depocenters. By linking the evolution of the continental margins to that of their African hinterland, this study bears important implications for the interplay of long-wavelength deformation and sediment transfers over paired shield-continental margin systems.

INTRODUCTION

The equatorial Atlantic Ocean opened as a consequence of oblique divergence along what were to become the best known examples of transform and oblique continental margins of northern South America and West Africa (Emery et al., 1975; Mascle and Blarez, 1987; Basile et al., 2005; Figs. 1 and 2). Those margins belonged to a large-scale network of rifts that led to the final dispersion

of the Gondwana supercontinent by breakup between South America and Africa during the Early Cretaceous (Fig. 1). Counterclockwise rotation of the African plate produced a northward rift propagation leading to the formation of the South Atlantic Ocean under dominantly normal divergence, whereas the future equatorial Atlantic domain underwent dextral-oblique divergence (e.g., Moulin et al., 2009; Frizon de Lamotte et al., 2015). The intracontinental African rifts, which were connected to the southern Atlantic and equatorial rift systems by a triple junction, aborted before the African continent could split into three subplates along the Western and Central rift system (Burke and Whiteman, 1973; Fairhead, 1988; Binks and Fairhead, 1992; Guiraud and Maurin, 1992; Fig. 1).

Given their transform character, the margins of the equatorial Atlantic Ocean were mainly investigated through the kinematics of ocean opening (e.g., Basile et al., 2005; Moulin et al., 2009; Heine et al., 2013; Basile, 2015) with an emphasis on the fracture zones and the vertical movements induced along the margins (Bouillin et al., 1998; Clift et al., 1998; Bigot-Cormier et al., 2005; Mercier de Lépinay, 2016). The abruptness of the equatorial margins of Africa results from the strong control of strike-slip faults (i.e., future transforms) during rifting. These steep margins have specific thermal and subsidence histories that are not yet well understood but are crucial in controlling—and unravelling—their high hydrocarbon potential (MacGregor et al., 2003). Published exploration studies have provided insights (Delteil et al., 1974; Kjemperud et al., 1992; Bennett and Rusk, 2002; MacGregor et al., 2003) but only at the scale of individual subbasins and/or along cross sections that do not allow apprehending the fully three-dimensional nature of the tectonostratigraphic evolution of the margins.

Integrated regional studies linking the stratigraphic history of the equatorial Atlantic margins to their deformation since pre-rift configuration are still lacking. Such studies require structural and paleogeographic reconstructions (i.e., maps showing past depositional environments) of their adjoining continental domain in order to address the coupling between margin evolution and the erosional, depositional, and deformational history of their hinterland in a “source-to-sink” perspective. So far, paleogeographic reconstructions for northwestern Africa did not include the equatorial margin domain (Guiraud

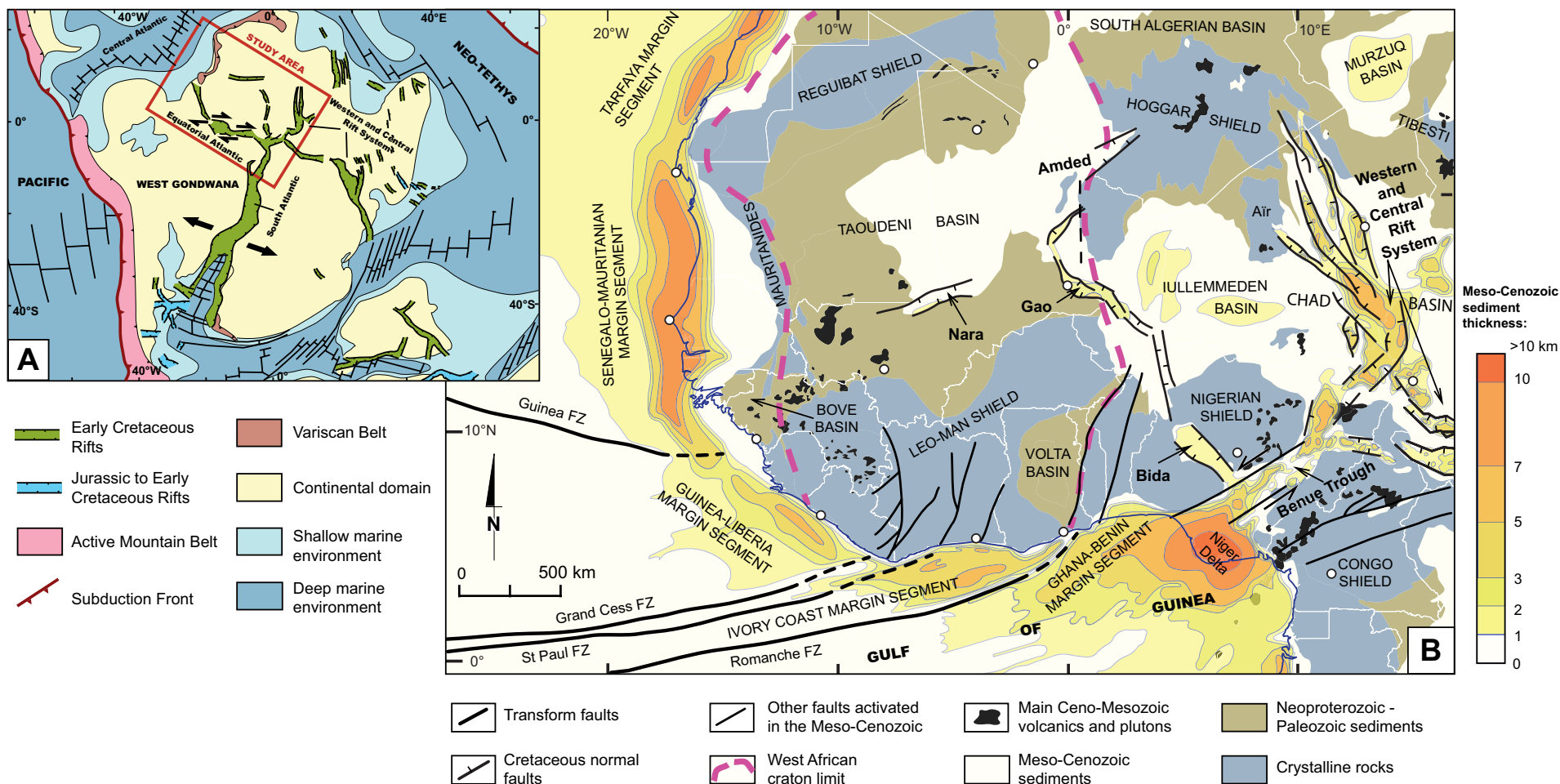


Figure 1. (A) Map showing the African and South American rift systems at ca. 120 Ma during dispersal of Gondwanaland (modified after Frizon de Lamotte et al., 2015). (B) Structural map of northwestern Africa showing Meso-Cenozoic faults and sedimentary basins (modified after Kogbe, 1981, and Milesi et al., 2010). Geologic contours are simplified from Figure 2. The names of the main Early Cretaceous intracontinental rifts are indicated (bold font). The frame of Figure 1B is shown in red on Figure 1A.

et al., 2005). Furthermore, those paleogeographic reconstructions were biased from a methodological viewpoint. Indeed, they often consider the preservation limits of sedimentary deposits of a given age as the limits of the sedimentation area of that age. Such is never the case, however, because the edges of coastal and intracratonic basins undergo erosion that leads to significant reduction of their original extent (Sloss, 1963).

In this contribution, we reassess the Meso-Cenozoic geological evolution of the Atlantic margins of northwestern Africa and their hinterland (south

of 28°N, west of 17°E) as well as the conjugate equatorial margin of northern South America (Fig. 1). Our work is based on a series of large-scale, off-shore-onshore geologic cross sections and nine maps showing successive geological configurations since 200 Ma, taking into account (1) restoration of the position of northern South America relative to northwestern Africa, (2) fault patterns and magmatic occurrences, (3) extent of erosion and/or sedimentation areas and associated depositional environment of sediments, and (4) constraints provided by low-temperature thermochronology data on the

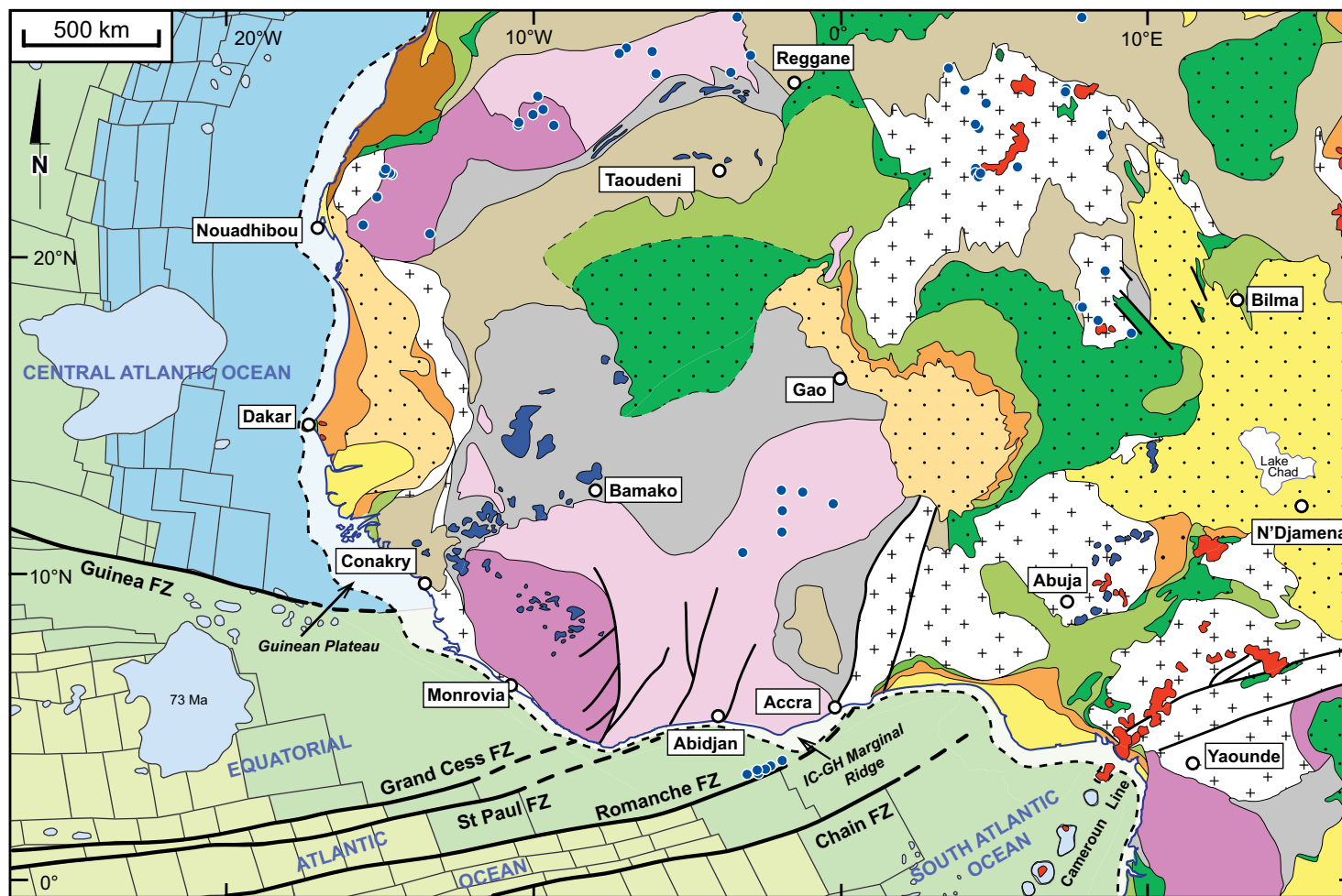
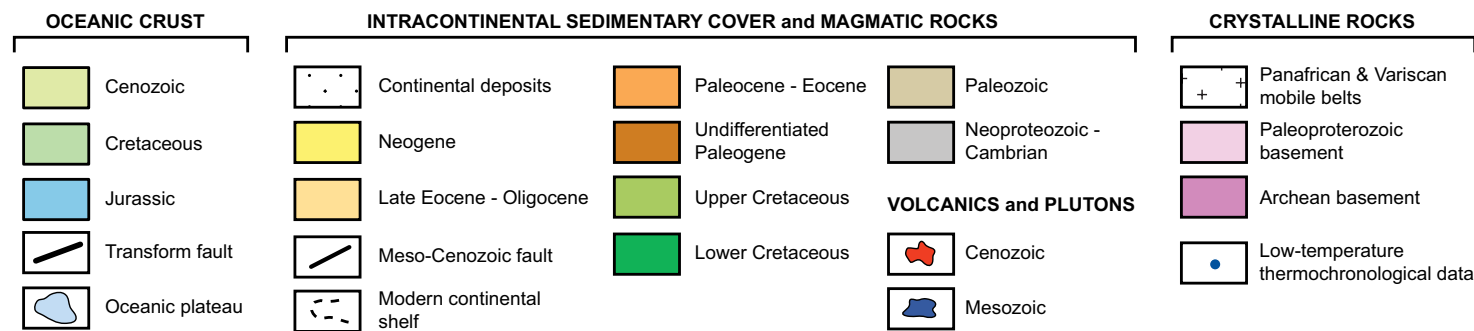


Figure 2. Simplified geologic map of West Africa compiled from Choubert and Fauremuret (1988), Fabre et al. (1996), Milesi et al. (2010), and this work. Quaternary sand cover has been omitted, and small Triassic–Jurassic sedimentary outcrops in the Tim Mersoi basin were included in Lower Cretaceous sediment map units. Lower Cretaceous and Paleogene continental sediments are grouped as the “Continental Intercalaire” and “Continental Terminal,” respectively. Only outcropping faults that were potentially activated during the Meso-Cenozoic are shown. Sources for low-temperature thermo-chronological data shown on the map are listed in Table 1. The equatorial Atlantic Ocean is considered as the oceanic lithosphere between the Guinea fracture zone in the north (boundary with the Central Atlantic Ocean) and the Chain fracture zone in the south (boundary with the South Atlantic Ocean). FZ—fracture zone.



burial or erosion of specific areas. Our work is based on a compilation of original geological source data from the literature, as well as seismic and well data along the continental margins. A specificity of our approach is that we evaluated the potential original minimal extent of sedimentary deposits for coastal and intracratonic basins beyond the present-day erosional limit of those basins. We provide a new evolving integrated structural and/or sedimentary offshore-onshore scheme at a subcontinental scale. Our compilation further allows proposing a new pre-rift fit between South America and northwestern Africa as well as a new synrift kinematic framework integrating mainland African rifts and the future margins. Our study opens a new perspective for linking the evolution of margins to intracratonic long-wavelength deformation and erosion and/or deposition patterns, with implications for paired shield-margin source-to-sink systems.

■ GEOLOGICAL OUTLINE AND EARLIER WORKS

The West African lithosphere mainly consists of an Archean–Paleoproterozoic nucleus (i.e., the West African craton), fringed by Pan-African (late Neoproterozoic) and Variscan (late Paleozoic) mobile belts (Figs. 1 and 2). Meso-Cenozoic sediments are preserved in several intracratonic basins around the Hoggar shield (Fig. 2). Those basins (namely, the Taoudeni, South Algerian, Murzuq, Chad, and Iullemeden basins) developed either on Neoproterozoic–Paleozoic platform sequences or directly on the basements (Radier, 1959; Greigert, 1966; Busson and Cornée, 1991; Fabre et al., 1996; Davidson et al., 2000). Jurassic and mostly Lower Cretaceous intracratonic sediments have been grouped as the “Continental Intercalaire” (e.g., Dars, 1960; Lefranc, 1983; Lefranc and Guiraud, 1990; Mateer et al., 1992; Fig. 2). A Cretaceous rift system is preserved in inland West Africa, most of which is now buried under Upper Cretaceous and Cenozoic series: the Western and Central rift system in the Chad Basin, which extends up to East Africa, the Gao and Bida rifts in the Iullemeden Basin, and the Nara and Amded rifts in the Taoudeni basin (Radier, 1959; Dars, 1960; Bellion et al., 1984; Genik, 1992, 1993; Fabre et al., 1996; Zanguina et al., 1998; Figs. 1 and 2). The Upper Cretaceous sequences recorded mostly transgressions far inland (Reyment, 1980; Dufaure et al., 1984). Marine sedimentation is recorded repeatedly until the Late Paleocene–Early Eocene, particularly in the Iullemeden and Chad basins (e.g., Radier, 1959; Greigert, 1966; Kogbe, 1980; Reyment, 1980; Moody and Sutcliffe, 1991). Those series are overlain by fluvial sediments of the Late Eocene–Early Oligocene “Continental Terminal” (Lang et al., 1986, 1990; Chardon et al., 2016; Fig. 2). Intense weathering has affected West Africa since the Late Cretaceous and left relicts of lateritic paleolandscapes, which have been used for reconstructing denudation histories and drainage evolution of West Africa (Beauvais and Chardon, 2013; Chardon et al., 2016). The present-day West African drainage system has stabilized in the Early Oligocene, following the onset of hotspot-related growth of topographic massifs such as the Hoggar and the Tibesti (Chardon et al., 2016), which led to the basin-and-swallow physiography of the continent (Burke, 1996).

The inland rift system is temporally and kinematically linked to the development of the equatorial Atlantic margin of Africa (Guiraud and Maurin, 1992), which may be divided into three segments separated by transforms (the Guinea-Liberia, Ivory Coast, and Ghana-Benin segments; Fig. 1). The current views on the opening of the equatorial Atlantic Ocean are summarized as follows (e.g., Popoff, 1988; MacGregor et al., 2003; Basile et al., 2005; Brownfield and Charpentier, 2006). The synrift stage begins in the Neocomian by transcurrent and extensional faulting (Fig. 1). Grabens of the Ghana-Benin margin segment are filled by Barremian–Aptian continental conglomerates, sandstones, and siltstones (Kjemperud et al., 1992; Chierici, 1996), which are overlain by Albian marine sandstones, black shales, and minor limestones (Chierici, 1996). The end of synrift deformation is marked by a regional unconformity underlying a latest Albian–Cenomanian marine series called the breakup unconformity. It is defined as an erosional surface formed at the end of intracontinental rifting and preceding seafloor spreading. This surface seals the synrift faults and underlies relatively undeformed postrift strata. The breakup unconformity is also documented on the conjugate Brazilian margins (Trosdorf Junior et al., 2007; Zalán and Matsuda, 2007; Soares Júnior et al., 2011). The kinematic model for the opening of the equatorial Atlantic Ocean is still under discussion, because of the “Cretaceous Magnetic Quiet” period and the difficulty to restore synrift structures (Moulin et al., 2009; Heine et al., 2013). Regression and transgression cycles and tectonic reactivation affected the African equatorial Atlantic margin during the postrift stage. At least two regional unconformities are identified on the Ivory Coast and Ghana-Benin margin segments; one is dated to the Senonian (Coniacian to Maastrichtian) and the other to the Oligocene (Simon and Amakou, 1984; Grillot et al., 1985; Chierici, 1996).

■ DATA AND METHOD

We established four large-scale, onshore-offshore cross sections over the study area in order to visualize the spatial relationships among inland sedimentary basins and continental margins (Fig. 3). These cross sections complement the paleomaps, which were established for specific periods matching known geodynamic events such as the emplacement of magmatic provinces, the continental rifting, or global transgression and regression cycles. In this study, we refer to the geologic time scale of Walker et al. (2012).

Integration of the Sedimentary Record

We first mapped the boundaries of the preserved sediments deposited during each time step. Stratigraphy, lithology, and paleoenvironment of these deposits (both at the surface and subsurface) have been compiled from published literature reporting first-hand data, observations, and maps (Table 1). Additional information was obtained along the African equatorial Atlantic margin and in the Gao rift (Fig. 1) from seismic and well data (~1000 seismic-reflection lines and 70 exploration wells, covering an area of more than 2×10^5 km² along the margin). For South American basins, we used essentially published studies and strati-

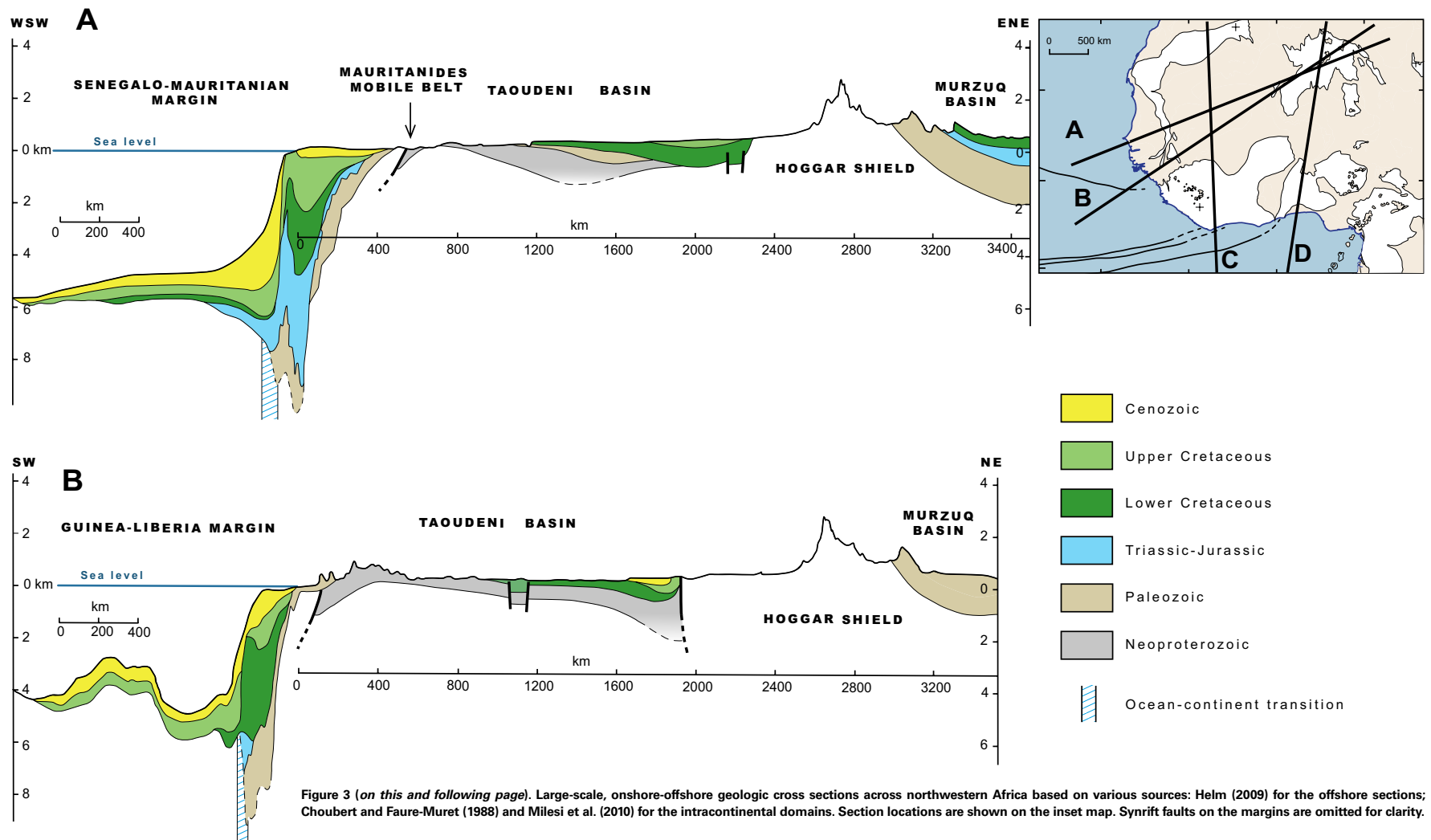


Figure 3 (on this and following page). Large-scale, onshore-offshore geologic cross sections across northwestern Africa based on various sources: Helm (2009) for the offshore sections; Choubert and Faure-Muret (1988) and Milesi et al. (2010) for the intracontinental domains. Section locations are shown on the inset map. Synrift faults on the margins are omitted for clarity.

graphic charts of Petrobras (Conde et al., 2007; Figueiredo et al., 2007; Pessoa Neto et al., 2007; Trostdorf Junior et al., 2007; Zalán, 2007; Zalán and Matsuda, 2007). Depositional environments of sediments are grouped in four categories: nonmarine and/or continental, transitional, shallow marine, and deep marine. Shallow-marine sediments are defined as shallower than 200 m depth (i.e., shelf sediments) and deep-marine sediments as deeper (continental slope and basin sediments). Transitional environments are coastal, lagoonal, estuarine, and/or deltaic sedimentary environments with near sea-level elevation. Avail-

able paleocurrent measurements are also indicated, which are mainly used to infer drainage direction and sense in alluvial settings. The present-day extent of preserved sedimentary deposits is hypothetical when strata are covered by younger deposits and are only revealed by seismic and well data. Nonmarine deposits of the "Continental Intercalaire" are usually poorly dated. Therefore, only uncertain (dashed) boundaries have been represented in those cases.

The limits of coastal and especially intracratonic basins are usually erosional. Erosion generally removes deposits along basin fringes as a con-

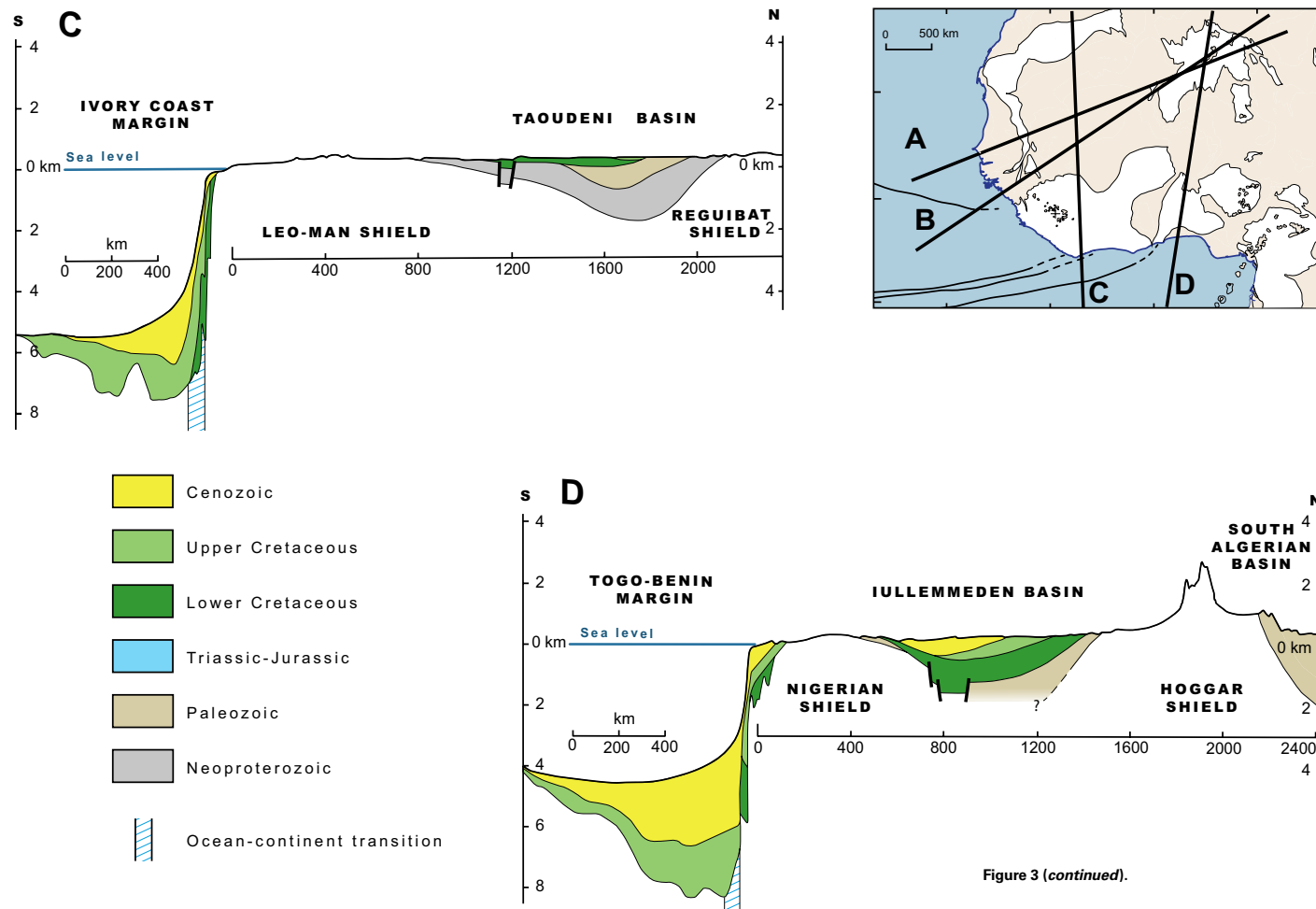


Figure 3 (continued).

sequence of flexural uplift of basin edges accompanying subsidence and sediment accumulation (Sloss and Scherer, 1975; Watts, 2001; Fig. 4A). The preserved deposits therefore only represent the minimum extent of the deposits at the time they were emplaced. This has led to a methodological limitation of paleogeographic studies, which usually mistake the extent of preserved sediments for their depositional area. In this study, we have assessed the potential minimum areal extent of sedimentary basins by estimating the map width of the subsequent erosion they have undergone at their margins. Let us consider ΔZ as the denudation due to a drop in base level consecutive to an uplift and/or a sea-level fall from time T1 to T2. E is the resulting inward (i.e., toward the basin interior) retreat of the basin's edges, and S is the topographic slope of the basin's margin (Fig. 4B). E_i and S_i and E_s and S_s are defined for

the inlandward slope of intracratonic basins and the seaward slope of coastal basins, respectively (Fig. 4B). Assuming a negligible short-wavelength relief, which is reasonable for cratonic surfaces and their marginal upwarps, $E = \Delta Z/S$.

The compilation of present-day continental topography of Africa reveals that regional seaward slopes (S_s) range from 1‰ to 2‰, and the regional inlandward slopes (S_i) range from 0.1‰ to 0.3‰. Those values may be reasonably taken as representative of past continental slope given the variety of morphotectonic contexts around today's African continent. Values of ΔZ in continental interiors may be constrained from denudation estimates derived from geomorphology and low-temperature thermochronology. Denudation of the Leo-Man shield (Figs. 1 and 2) is estimated at 2–15 m/Ma for the Cenozoic, based on incision of dated lateritic relict landscapes (Beauvais

TABLE 1. REFERENCES USED FOR THE GEOLOGICAL RECONSTRUCTIONS

| Thematic geological items | References | Paleogeographic maps | | | | | | | | |
|--|--------------------------------|----------------------|------------|------------|------------|----------|-----------|-----------|-----------|-----------|
| | | 235–190 Ma | 140–133 Ma | 120–115 Ma | 107–100 Ma | 97–93 Ma | 86–84 Ma | 72–66 Ma | 61–56 Ma | 34–23 Ma |
| | | Figure 5 | Figure 6 | Figure 7 | Figure 8 | Figure 9 | Figure 10 | Figure 11 | Figure 12 | Figure 13 |
| SEDIMENTARY RECORD | | | | | | | | | | |
| Intracontinental Africa | | | | | | | | | | |
| Taoudenni Basin (including the Nara and Amded rifts) | Fabre et al., 1996 | | x | x | x | x | x | | | |
| | Fabre, 2005 | | x | x | x | x | x | | | |
| | Bellion et al., 1984 | | x | | | | | | | |
| | Cornet, 1943 | | x | x | x | | | x | x | x |
| | Busson, 1971 | | | x | x | | x | x | x | |
| | Dars, 1960 | | x | x | x | | | x | x | x |
| | Choubert and Faure-Muret, 1988 | | x | x | x | | | | | |
| Iullemeden Basin (including the Gao and Kandi rifts) | Greigert, 1966 | | x | x | x | x | | x | x | x |
| | Greigert and Pougnet, 1967 | | x | x | x | x | | x | x | x |
| | Chardon et al., 2016 | | | | | | | | x | x |
| | Kogbe, 1981 | | x | x | x | | | x | x | x |
| | Valsardieu, 1971 | x | x | x | x | | | | | |
| | Radier, 1959 | | | | | | | x | x | x |
| | Mateer et al., 1992 | | | x | x | | | | | |
| | Zanguina et al., 1998 | x | x | x | x | x | x | x | x | |
| | Moody and Sutcliffe, 1991 | | x | x | x | x | | x | | |
| | Alidou and Lang, 1983 | | x | x | x | | | | | x |
| Alidou et al., 1991 | | x | x | x | | | | | x | |
| Chad Basin (including the Western Central African rift system) | Genik, 1992, 1993 | x | x | x | x | x | x | x | x | x |
| | Choubert and Faure-Muret, 1988 | | x | x | x | x | x | x | x | x |
| | Greigert and Pougnet, 1967 | | x | x | x | x | x | x | x | x |
| | Zanguina et al., 1998 | | x | x | x | x | x | x | x | x |
| | Avbovo et al., 1986 | | | | x | x | x | x | x | x |
| Murzuq Basin | Davidson et al., 2000 | x | x | x | x | | | | | |
| | Klitzsch, 2000 | x | x | x | x | | | | | |
| | Dufaure et al., 1984 | | | | | | | x | | |
| Benue Trough | Benkheilil et al., 1988 | | | x | x | x | | x | x | |
| | Benkheilil, 1989 | | | x | x | x | | x | x | |
| | Allix, 1983 | | | x | x | x | | x | x | |
| | Allix and Popoff, 1983 | | | x | | | | | | |
| | Allix et al., 1981 | | | x | | | | | | |
| | Jermannaud et al., 2010 | | | | | | | | | x |
| | Petters, 1980, 1983 | | | x | x | x | | x | x | |
| | Popoff, 1988 | | x | x | x | | | | | |
| Sokari, 1992 | | | x | x | | | | | | |
| Bida Rift | Akande et al., 2005 | | | | | | | x | | |
| | Ojo and Akande, 2009 | | | | | | | x | | |
| | Agyingi, 1993 | | | | | | | x | | |
| Leo-Man Shield (weathering record) | Grimaud et al., 2015 | | | | | | | | x | x |
| | Chardon et al., 2016 | | | | | | | | x | x |
| | Beauvais et al., 2008 | | | | | | | | x | x |
| | Beauvais and Chardon, 2013 | | | | | | | | x | x |

(continued)

TABLE 1. REFERENCES USED FOR THE GEOLOGICAL RECONSTRUCTIONS (*continued*)

| Thematic geological items | References | Paleogeographic maps | | | | | | | | |
|--|----------------------------------|----------------------|------------|------------|------------|----------|-----------|-----------|-----------|-----------|
| | | 235–190 Ma | 140–133 Ma | 120–115 Ma | 107–100 Ma | 97–93 Ma | 86–84 Ma | 72–66 Ma | 61–56 Ma | 34–23 Ma |
| | | Figure 5 | Figure 6 | Figure 7 | Figure 8 | Figure 9 | Figure 10 | Figure 11 | Figure 12 | Figure 13 |
| SEDIMENTARY RECORD (<i>continued</i>) | | | | | | | | | | |
| Atlantic margins | | | | | | | | | | |
| Tarfaya Basin | Leprêtre, 2015 | | x | x | x | x | x | x | x | x |
| | Davison, 2005 | x | x | x | x | x | x | x | x | x |
| | Baby et al., 2014 | | x | | | | | x | | |
| Senegalo-Mauritanian Basin | Baby, 2012 | x | x | x | x | x | x | x | x | x |
| | Baby et al., 2014 | x | x | x | x | x | x | x | x | x |
| | Davison, 2005 | x | x | x | x | x | x | x | x | x |
| | Tari et al., 2003 | x | x | x | x | x | x | x | x | x |
| | Brownfield and Charpentier, 2003 | x | x | x | x | x | x | x | x | x |
| Eastern North America | Olsen, 1997 | x | | | | | | | | |
| Guinea and Demerara Plateau | Dumestre and Carvalho, 1985 | x | x | x | x | x | x | x | x | x |
| | Stoecklin, 1987 | | x | x | x | x | x | x | x | x |
| | Marinho, 1985 | x | x | x | x | x | x | x | x | x |
| | Benkheilil et al., 1995 | | x | x | x | | | | | |
| Equatorial Atlantic margins | This study | | | x | x | x | x | x | x | x |
| | Gouyet, 1988 | | x | x | x | | | | | |
| | Benkheilil et al., 1995 | | x | x | x | | | | | |
| | Da Costa et al., 2009 | | | | | | | x | x | x |
| | Yang and Escalona, 2011 | | x | x | x | | | | | |
| | Figueiredo et al., 2007 | x | x | x | x | x | x | | | |
| | Zalán and Matsuda, 2007 | | x | x | x | x | | | | |
| | Soares et al., 2007 | | | x | x | x | x | | | |
| | Zalán, 2007 | | | x | x | x | x | x | | |
| | Trosdorf Junior et al., 2007 | | | x | x | x | x | x | | |
| | Conde et al., 2007 | | | x | x | x | x | x | | |
| | Pessoa Neto et al., 2007 | | x | x | x | x | x | x | | |
| Soares Junior et al., 2011 | x | x | x | x | x | | | | | |
| South Atlantic margins | Chaboureau, 2012 | | x | x | | | | | | |
| | Chaboureau et al., 2013 | | x | x | | | | | | |
| | Seranne and Anka, 2005 | | | | | x | x | x | x | x |
| Intracontinental Northern South America | | | | | | | | | | |
| | Cunha et al., 2007 | | | x | x | x | | | | |
| | Costa et al., 2001 | | | x | x | x | | | | |
| | Vaz et al., 2007a | x | | x | x | x | | | | |
| | Vaz et al., 2007b | x | x | x | | | | | | |
| | Assine, 2007 | | x | | x | | | | | |
| | de Matos, 1992 | | x | | x | | | | | |

(*continued*)

TABLE 1. REFERENCES USED FOR THE GEOLOGICAL RECONSTRUCTIONS (*continued*)

| Thematic geological items | References | Paleogeographic maps | | | | | | | | |
|--------------------------------------|-------------------------------|----------------------|------------|------------|------------|----------|-----------|-----------|-----------|-----------|
| | | 235–190 Ma | 140–133 Ma | 120–115 Ma | 107–100 Ma | 97–93 Ma | 86–84 Ma | 72–66 Ma | 61–56 Ma | 34–23 Ma |
| | | Figure 5 | Figure 6 | Figure 7 | Figure 8 | Figure 9 | Figure 10 | Figure 11 | Figure 12 | Figure 13 |
| FAULT PATTERNS AND KINEMATICS | | | | | | | | | | |
| Intracontinental Africa | | | | | | | | | | |
| Amded rift | Fabre et al., 1996 | | x | x | x | | | | | |
| | Dars, 1960 | | x | x | x | | | | | |
| Nara rift | Dars, 1957; Dars, 1960 | | x | x | x | | | | | |
| | Bellion et al., 1984 | | x | x | x | | | | | |
| Gao rift | This study | | | x | x | | | | | |
| Western Central African rift system | Genik, 1992, 1993 | | x | x | | | x | x | x | |
| | Zanguina et al., 1998 | | x | x | | | x | x | x | x |
| | Guiraud and Bosworth, 1997 | | | | | | x | | | |
| | Loule and Pospisil, 2013 | | | x | | x | x | x | | |
| | Guiraud and Maurin, 1992 | | | | | | | x | | |
| | Le Marechal and Vincent, 1972 | | | x | x | x | | | | |
| Bida rift | Ngangom, 1983 | | x | x | x | | | | | |
| | Kogbe et al., 1983 | | | | | | | | x | |
| Benue Trough | Ojo and Ajakaiye, 1976 | | | | | | | | x | |
| | Benkhelil, 1988 | | | x | x | | x | x | | |
| Benue Trough | Benkhelil et al., 1989 | | | x | x | | x | x | | |
| | Allix et al., 1984 | | | x | x | | x | x | | |
| | Benkhelil and Guiraud, 1980 | | | x | x | | x | x | | |
| | Guiraud, 1993 | | x | x | x | | | x | | |
| | | | | | | | | | | |
| Atlantic margins | | | | | | | | | | |
| Central Atlantic margins | Withjack et al., 1998 | x | | | | | | | | |
| | Le Roy and Pique, 2001 | x | | | | | | | | |
| | Labails, 2007 | x | | | | | | | | |
| Guinea and Demerara plateaus | Benkhelil et al., 1995 | | x | x | x | | | | | |
| | Sapin et al., 2016 | | x | x | x | | | | | |
| | Marinho et al., 1988 | | x | x | x | | | | | |
| Equatorial Atlantic margins | This study | | | x | x | x | x | x | | |
| | Basile et al., 2013 | | x | x | x | | | | | |
| | Benkhelil et al., 1995 | | x | x | x | | | | | |
| | Sapin et al., 2016 | | x | x | x | | | | | |
| | Soares Junior et al., 2008 | | x | x | x | | | | | |
| | Soares Junior et al., 2011 | x | x | x | x | | | | | |
| South Atlantic margins | Chaboureaux, 2012 | | x | x | | | | | | |
| | Chaboureaux et al., 2013 | | x | x | | | | | | |
| | Turner et al., 2003 | | x | x | | | | | | |
| Inland Northern South America | | | | | | | | | | |
| Inland Northern South America | Vaz et al., 2007b | x | x | x | | | | | | |
| | Assine, 2007 | | x | | x | | | | | |
| | de Matos, 1992 | | x | | x | | | | | |

(continued)

TABLE 1. REFERENCES USED FOR THE GEOLOGICAL RECONSTRUCTIONS (continued)

| Thematic geological items | References | Paleogeographic maps | | | | | | | | |
|--|-----------------------------|----------------------|------------|------------|------------|----------|-----------|-----------|-----------|-----------|
| | | 235–190 Ma | 140–133 Ma | 120–115 Ma | 107–100 Ma | 97–93 Ma | 86–84 Ma | 72–66 Ma | 61–56 Ma | 34–23 Ma |
| | | Figure 5 | Figure 6 | Figure 7 | Figure 8 | Figure 9 | Figure 10 | Figure 11 | Figure 12 | Figure 13 |
| LOW-TEMPERATURE THERMOCHRONOLOGICAL CONSTRAINTS | | | | | | | | | | |
| Northwestern Africa | | | | | | | | | | |
| | Leprêtre et al., 2014 | x | x | x | x | x | x | x | x | x |
| | Leprêtre, 2015 | x | x | x | x | x | x | x | x | x |
| | Leprêtre et al., 2015 | x | x | x | x | x | x | x | x | x |
| | Gunnell, 2003 | x | x | x | x | x | x | x | x | x |
| | Rougier, 2012 | | | | | x | x | x | x | x |
| | Rougier et al., 2013 | | | | | x | x | x | x | x |
| | Cavellec, 2006 | | | | | x | x | x | x | x |
| | English et al., 2016 | | x | x | x | x | x | x | x | x |
| | Bigot-Cormier et al., 2005 | | | | x | x | x | | | |
| | Clift et al., 1997, 1998 | | | | x | x | x | x | x | x |
| | Bouillin et al., 1997, 1998 | | | | x | x | x | x | x | x |
| Northern South America | | | | | | | | | | |
| | Harman et al., 1998 | x | x | x | | | | | | |
| | De Morais Neto et al., 2006 | x | x | x | x | | | | | |
| | De Morais Neto et al., 2008 | x | x | x | x | | | | | |
| | Turner et al., 2008 | | | x | | | | | | |

Supplemental File 1, to accompany Geosphere paper "Paleogeographic and structural evolution of northwestern Africa and its Atlantic margins since the early Mesozoic" by Ye et al.

Table S1. Compilation of thermochronological data (Apatite Fission Track analysis (AFTA) and Apatite (U-Th-Sm)/He dating (AHe) data) available over Northwestern Africa. Sample's name, location, lithology, age and mean track length (based from AFTA, AHe data) and the corresponding reference are shown for each sample, when available. The reader may access the temperature-time paths obtained by data inversion by consulting the cited studies.

| Sample | Lat | Lon | Location | Lithology | Age (Ma) | TL (μm) | TL _{95%} (μm) | TL _{5%} (μm) | TL _{50%} (μm) | Reference |
|---------|-------|-------|----------|-------------|----------|---------|------------------------|-----------------------|------------------------|-----------|
| TC00110 | 9.89 | 24.26 | Chargha | granite | 100 | 11.9 | 6.2 | 1.7 | 104.53 | (11) |
| TC00119 | 9.49 | 24.26 | Chargha | granite | 100 | 11.9 | 6.2 | 1.7 | 104.53 | (11) |
| TC00118 | 10.58 | 24.76 | Chargha | granite | 100 | 10.4 | 6.2 | 2.1 | 103.88 | (11) |
| 197 | 7.26 | 26.28 | Chargha | metagranite | 98 | 9.4 | 6.3 | 1.8 | 101.86 | (5) |
| TC00685 | 10.58 | 24.26 | Chargha | metagranite | 172 | 13 | 11.7 | 6.3 | 2.0 | (11) |
| TC00120 | 9.76 | 24.26 | Chargha | granite | 100 | 12 | 12.4 | 6.2 | 1.8 | (11) |
| AC-21 | 7.26 | 26.28 | Chargha | granite | 102 | 18 | 13.0 | 6.2 | 1.8 | 28037 |
| TC00103 | 10.58 | 24.26 | Chargha | granite | 106 | 21 | 12.3 | 6.2 | 2.3 | 80-01 |
| 153 | 2.26 | 27.26 | Chargha | granite | 107 | 21 | 12.3 | 6.2 | 2.3 | 80-01 |
| 126 | 3.88 | 25.26 | Chargha | granite | 104 | 21 | 12.3 | 6.2 | 2.3 | 80-01 |
| 127 | 3.88 | 25.26 | Chargha | granite | 107 | 21 | 12.3 | 6.2 | 2.3 | 80-01 |

'Supplemental File 1. Compilation of published thermochronological data and Meso-Cenozoic magmatic occurrences over northwestern Africa. Please visit <http://doi.org/10.1130/GES01426.S1> or the full-text article on www.gsapubs.org to view the Supplemental File 1.

and Chardon, 2013; Grimaud et al., 2014, 2015) and 6–13 m/Ma for the Mesozoic based on low-temperature thermochronology (Gunnell, 2003). Assuming an average denudation rate of 9 m/m.y. over a 10 m.y. period (typical time increment between our successive paleomaps) yields a ΔZ value of 90 m. The preservation of shallow-marine sediments in coastal basins (deposited under less than 200 m of water) also provides another constraint on denudation at basin edges, implying maximum ΔZ of 200 m.

Figure 4C is an abacus showing the relationship between E and S for various values of ΔZ. Considering the mean regional slopes of 1‰–2‰ and 0.1‰–0.3‰ for Ss and Si, denudation-derived ΔZ of 90 m would correspond to values of 45–90 km and 300–900 km for Es and Ei, respectively (Fig. 4C). Considering a maximum sediment bathymetry-derived ΔZ of 200 m, the same regional slopes would yield maximum values of 100–200 km and >700 km for Es and Ei, respectively (Fig. 4C). The implication of these results is that the limits of intracratonic basins were typically located hundreds of km (≥300 km) beyond their preservation limit for a given time period. This distance comes down to tens of km (≤100 km) for coastal basins on oceanward continental slopes. Those distances were used as guidelines to draw the potential minimum original extent of sedimentation areas around preserved sediments. Paleocurrent and low-temperature thermochronological data have been used to further constrain those contours in a way that is described as follows.

Paleocurrent data help reconstruct paleoalluvial plains fragmented by uneven erosion. Indeed, let us consider paleocurrents measured in a paleo-allu-

vial plain sedimentary complex pointing to river flow outside the preserved limits of the alluvial complex, i.e., toward the exposed substrate of the alluvial complex, which may consist of basement or older sediments. Such a configuration implies that this substrate had to be flooded by the considered alluvial plain at the time the plain was functional.

Published data from apatite fission-track analysis and apatite (U-Th-Sm)/He dating help constrain thermal histories of samples residing in the first 3–4 km of the crust (Gallagher et al., 1998; Ehlers and Farley, 2003). Considering the non-orogenic context of West Africa and its margins, and in the cases where the samples were not affected by major thermal events, heating periods reflect burial under sediments, whereas cooling periods indicate dominant erosion-driven exhumation and therefore an eroding land surface above a considered sample. Published temperature-time paths obtained by data inversion have been used (Table 1; Fig. 2; see also Table S1 in Supplemental File 1). For the time step corresponding to each paleomap, heating or cooling sample locations are reported and are used semiquantitatively to further constrain the extent of areas submitted to dominant erosion or sedimentary burial. Samples undergoing rapid cooling and/or heating (cooling and/or heating rate higher than 1 °C/Ma) are distinguished from those undergoing slow cooling and/or heating. On the paleomaps, the original minimum extent of sedimentation areas is drawn in lighter color than the corresponding preserved deposits (Figs. 5–13). Conversely, continental areas mapped as exposed to erosion or sediment bypassing correspond to their maximum potential extent.

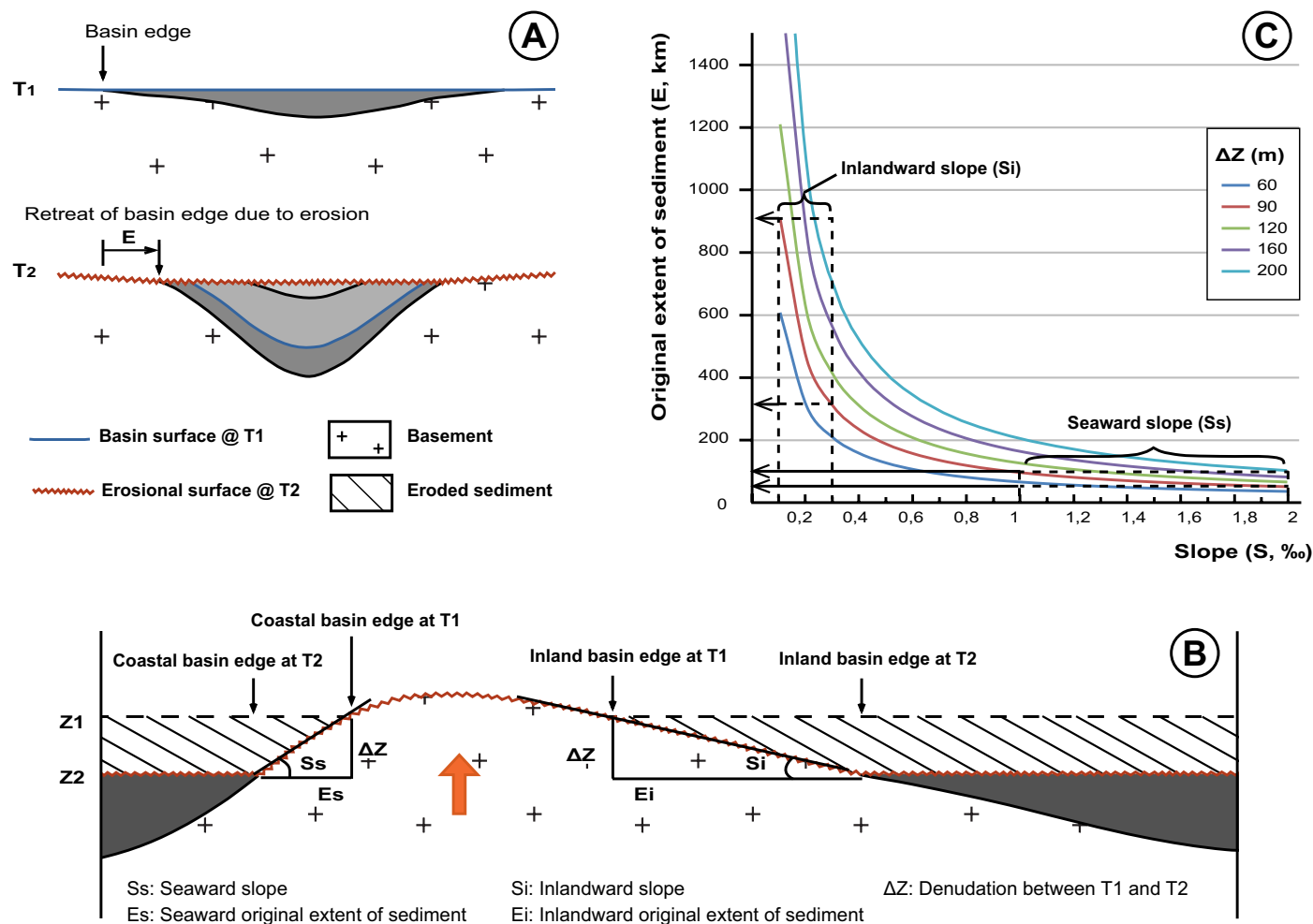


Figure 4. Estimation of the original minimum extent of sedimentary deposits at the edges of coastal and intracratonic basins. (A) Schematic illustration of the retreat (E) of an intracratonic basin edges between time T1 to T2 (modified after Sloss and Scherer, 1975). (B) Cross section of a marginal upwarp showing the influence of topographic slopes (S) on the original horizontal extent of sedimentary deposits and their erosion at basin edges. (C) Curves showing the relationships among the regional slope (S), the original extent of sediments (E), and denudation (ΔZ). See text for further explanations.

Fault Patterns

Tectonic structures active during the time step considered for each paleo-map are shown (e.g., normal faults bounding rifted basins, strike-slip faults, and anticlines and/or arches). The main criterion for mapping an active structure is based on the evidence for slip on a fault or amplification of an arch before, during, or after deposition of sediments of constrained age. Such an approach is particularly useful for documenting synrift sediments and fault reactivation. Such observations are mainly made on seismic lines, biostratigraphically calibrated by well data (mostly in marginal basins), and at some field localities.

The onset of rifting is not well constrained because only a few wells reached pre-rift strata. Moreover, rifting generally led to the accumulation of nonmarine sediments, which are not well dated except where lava flows are interbedded. Therefore, the dating of structures based on their relationships with the sediments may suffer some uncertainty. Such an uncertainty is taken into account by representing the active structures with a dashed line, indicating the actual location of the structure but a probable activity for the considered time slice (Figs. 5–13). Mapping of the structures is based on our own work for the equatorial margin of Africa and mainly on published works for the other margins and the intracontinental domains (Table 1).

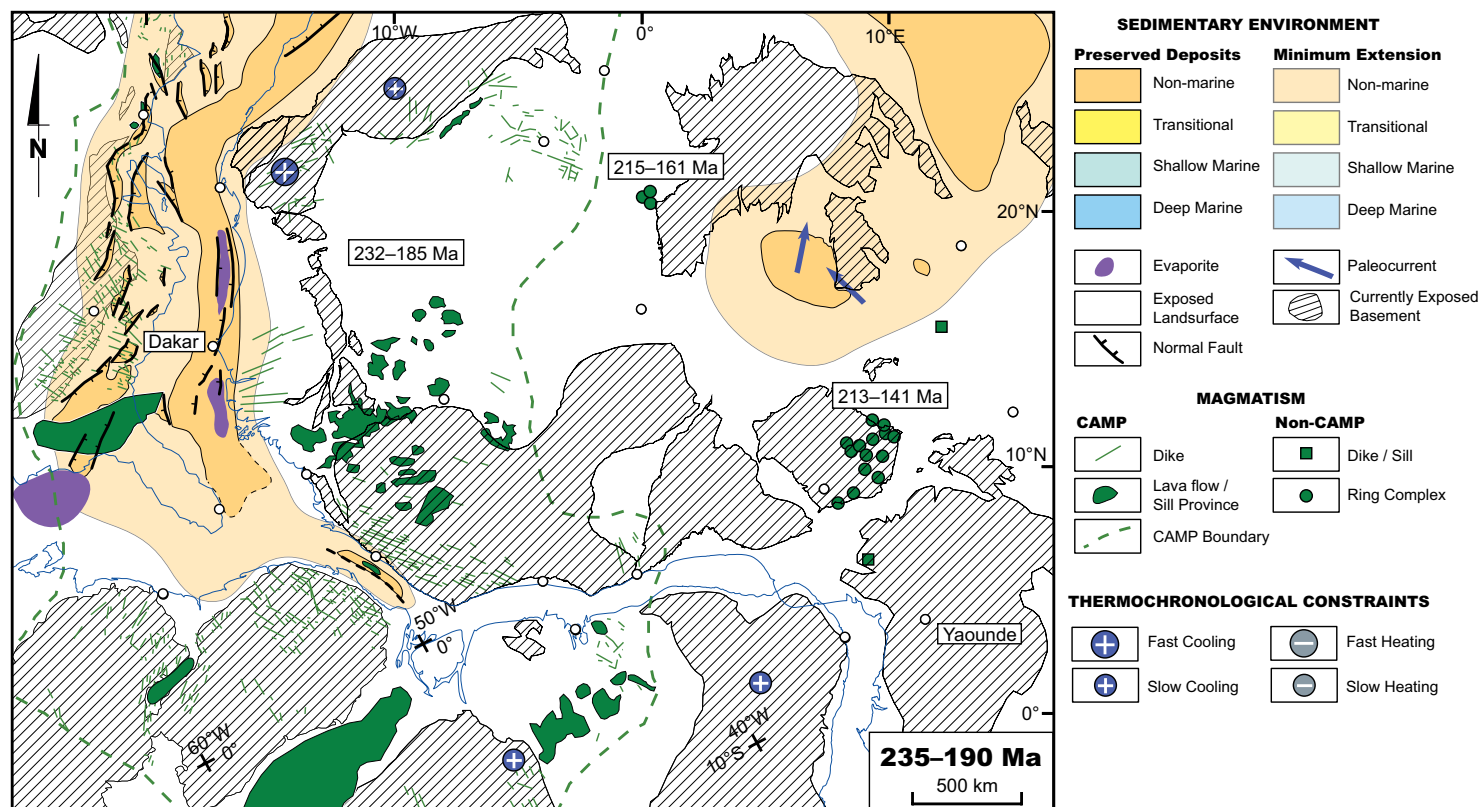


Figure 5. Geological configuration of northwestern Africa and adjoining North and South America during the Early Jurassic (235–190 Ma). Magmatic features of the Central Atlantic Magmatic Province (CAMP) are adapted from Jourdan et al. (2009). The age range of the magmatic clusters is indicated. The present-day shorelines of North America and northern South America (thin blue lines) are restored to their position relative to fixed Africa at the end of the considered time interval. Open circles are the localities from Figures 1B and 2.

Magmatism

We compiled and mapped the location, emplacement mode, age, and dating method of Meso-Cenozoic magmatic occurrences in West Africa and along its margins from literature (Figs. 5–13; Table S2 in Supplemental Item 1 [see footnote 1]). For northern South America, we used the synthesis of Mizusaki et al. (2002). Magmatic occurrences are categorized in lava flow, dike, sill, ring complex, kimberlite clusters, and kimberlite occurrences (Figs. 5–13).

Palinspastic and Kinematic Reconstruction

We adopted the kinematic models of the Atlantic Ocean opening proposed by Moulin et al. (2009) and Heine et al. (2013) for relative positioning of the current coastlines for each time interval. Heine et al. (2013) produced pre-litho-

spheric breakup (i.e., pre-oceanic lithosphere) reconstructions of the equatorial Atlantic domain from the Berriasian (145 Ma) to the late Albian (104 Ma) by using the GPlate software for paleotectonic reconstruction. Besides postrift seafloor magnetic anomalies, those reconstructions used published and confidential industrial data allowing for the quantification of rifting-related horizontal continental crustal deformation considering rift infill and fault patterns corrected from postrift subsidence (see Heine et al., 2013, for more details).

Moulin et al. (2009) suggest another pre-opening fit at 112 Ma, based mainly on correlations of structures across the equatorial Atlantic domain (magnetic lineaments, conjugate plateaus, and fracture zones), without considering synrift fault patterns and deformation. The pre-lithospheric breakup fit of Heine et al. (2013) appears to be more consistent with our synrift fault patterns on both the African and South American margins (see below), which must indeed develop within stretching continental crusts, assuming no major

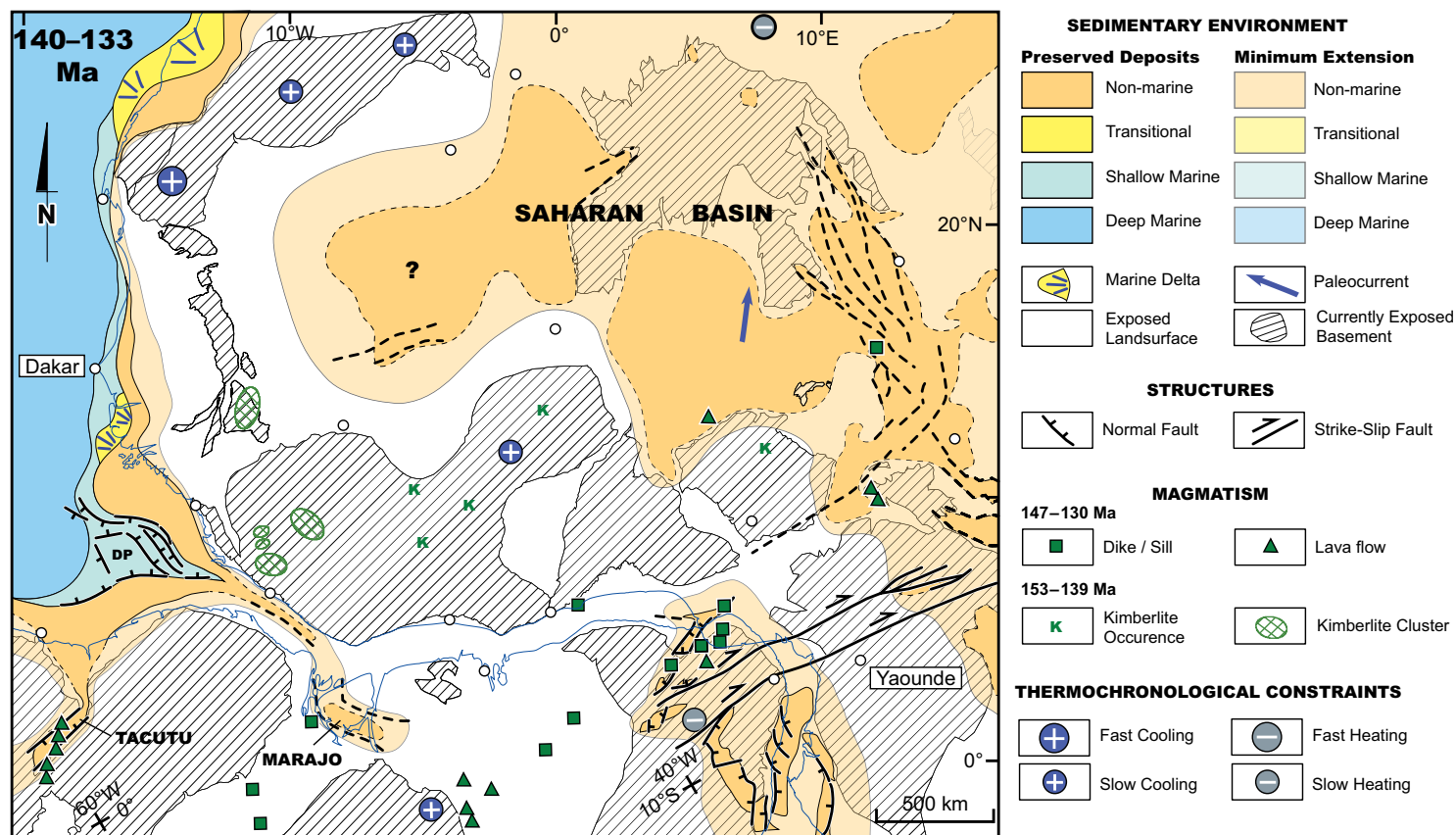


Figure 6. Geological configuration of northwestern Africa, adjoining South America, and the eastern Central Atlantic Ocean during the Valanginian (140–133 Ma). DP—Demerara plateau. Same conventions as in Figure 5.

postrift reactivation occurred. It also appears to better match what is known of the timing of the lithospheric breakup, i.e., in the late Albian (Dumestre and Carvalho, 1985; Kjemperud et al., 1992; Chierici, 1996). We therefore used the reconstructions of Heine et al. (2013) for the rifting stages from the Valanginian to the late Albian (140–97 Ma), and we adjusted them based on our new mapping of fault patterns. As for the postrift period, we adopted the model of Moulin et al. (2009) because the magnetic anomalies they used are well constrained, especially from 84 Ma (Chron 34) onward.

Given the biostratigraphic age uncertainties on the sediments, the sedimentary and structural features reported on each paleomap had to be integrated over a period of a few million years. The end of a given period is considered as the minimum age of each feature. The paleoposition of continental

masses shown on Figures 5–13 corresponds to that computed for the end of the time period considered for each map. An exception to that rule is the first paleomap (Fig. 5), which integrates magmatic occurrences that may be much older (up to 245 Ma) and younger (up to 140 Ma) than the palinspastic, paleogeographic, and structural reconstruction set at 190 Ma. This choice provides a picture of the widespread magmatism over northwestern Africa, before the rifting of the equatorial Atlantic domain, which implies that large areas were potentially submitted to uplift and erosion. The last paleomap (Oligocene; 34–23 Ma; Fig. 13) also displays Eocene to present-day magmatic occurrences. The remaining seven paleomaps correspond to Valanginian (140–133 Ma; Fig. 6), middle Aptian (120–115 Ma; Fig. 7), late Albian (107–100 Ma; Fig. 8), late Cenomanian (97–93 Ma; Fig. 9), Santonian (86–84 Ma; Fig. 10), Maas-

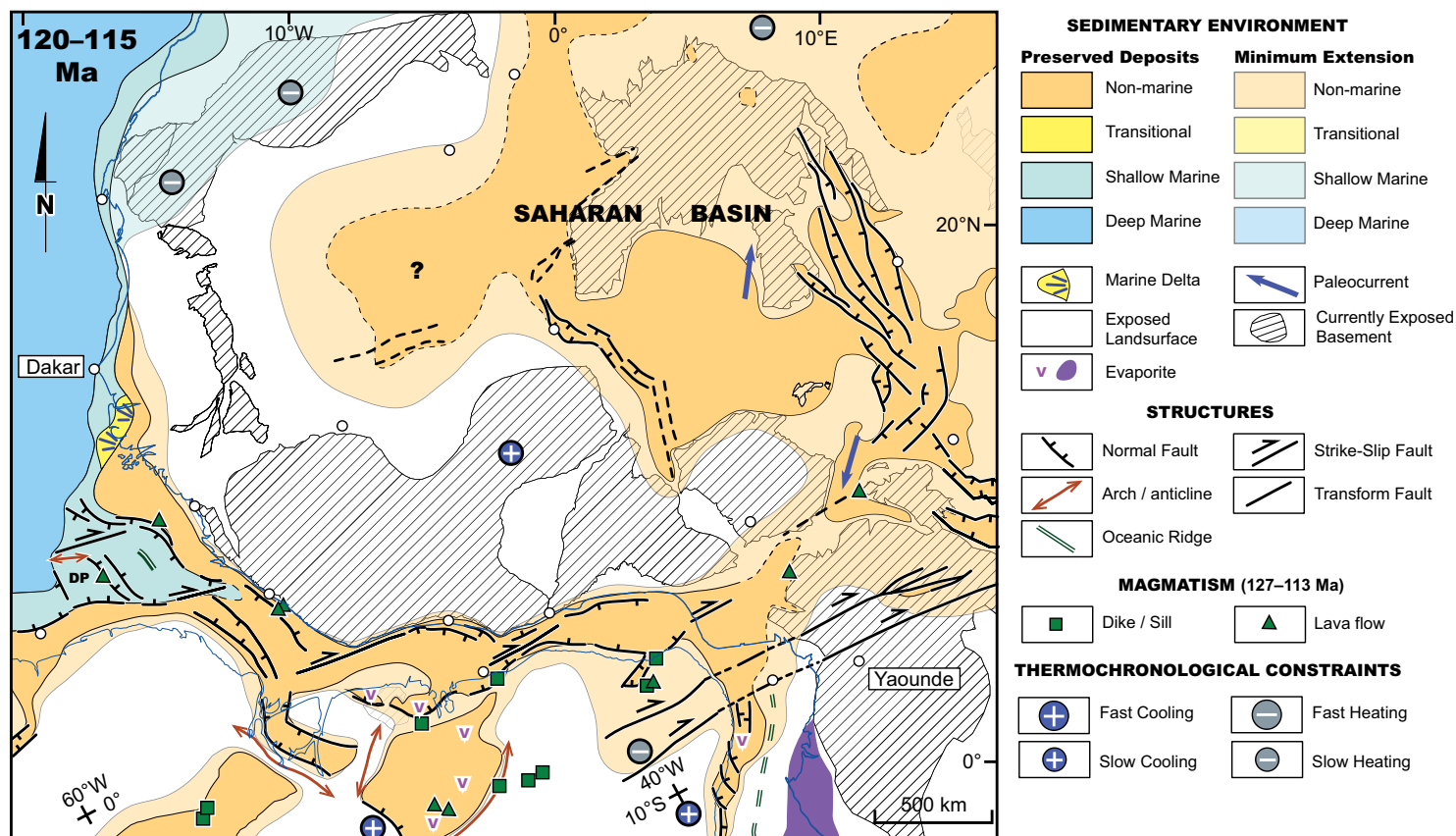


Figure 7. Geological configuration of northwestern Africa, adjoining South America, and the eastern Central Atlantic Ocean during the middle Aptian (120–115 Ma). DP—Demerara plateau. Same conventions as in Figure 5.

trichitan (72–66 Ma; Fig. 11), and Late Paleocene (61–56 Ma; Fig. 12). An animation of the paleomaps is available as Supplemental File 2². For specific localities, structures, or sedimentary basin locations, the reader may refer to Figures 1 and 2.

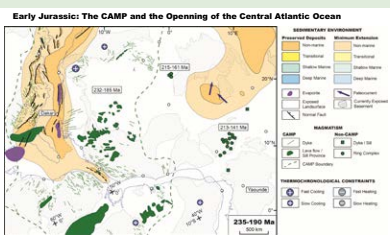
RESULTS AND INTERPRETATION

Cross Sections Linking the Marginal and Intracontinental Domain

The cross sections (Fig. 3) display the present-day configurations of onshore and offshore basins, basement highs, and their typical wavelengths. The geometry is spatially consistent across the Central Atlantic and

equatorial margins, with continental margin basins separated from intracratonic basins by a marginal upwarp. The inland basal unconformities of intracratonic basins roughly coincide with the slope of basement highs such as the Hoggar and Reguibat shields. The marginal upwarps are positive topographic features that form at the time of rifting and are sustained and/or reactivated afterwards (Gilchrist and Summerfield, 1990; Gallagher et al., 1995).

Considering only the Meso-Cenozoic sediments (that recorded continental surface evolution since the rifting of the Central Atlantic), the edges of intracratonic basins are erosional limits, resulting from the truncation of the strata on the inland slopes of the marginal upwarps. Similar truncations are expected, though on a shorter distance, at the coastal fringes of marginal basins



²Supplemental File 2. Animation of geologic paleomaps in PowerPoint format. Please visit <http://doi.org/10.1130/GES01426.S2> or the full-text article on www.gsapubs.org to view Supplemental File 2.

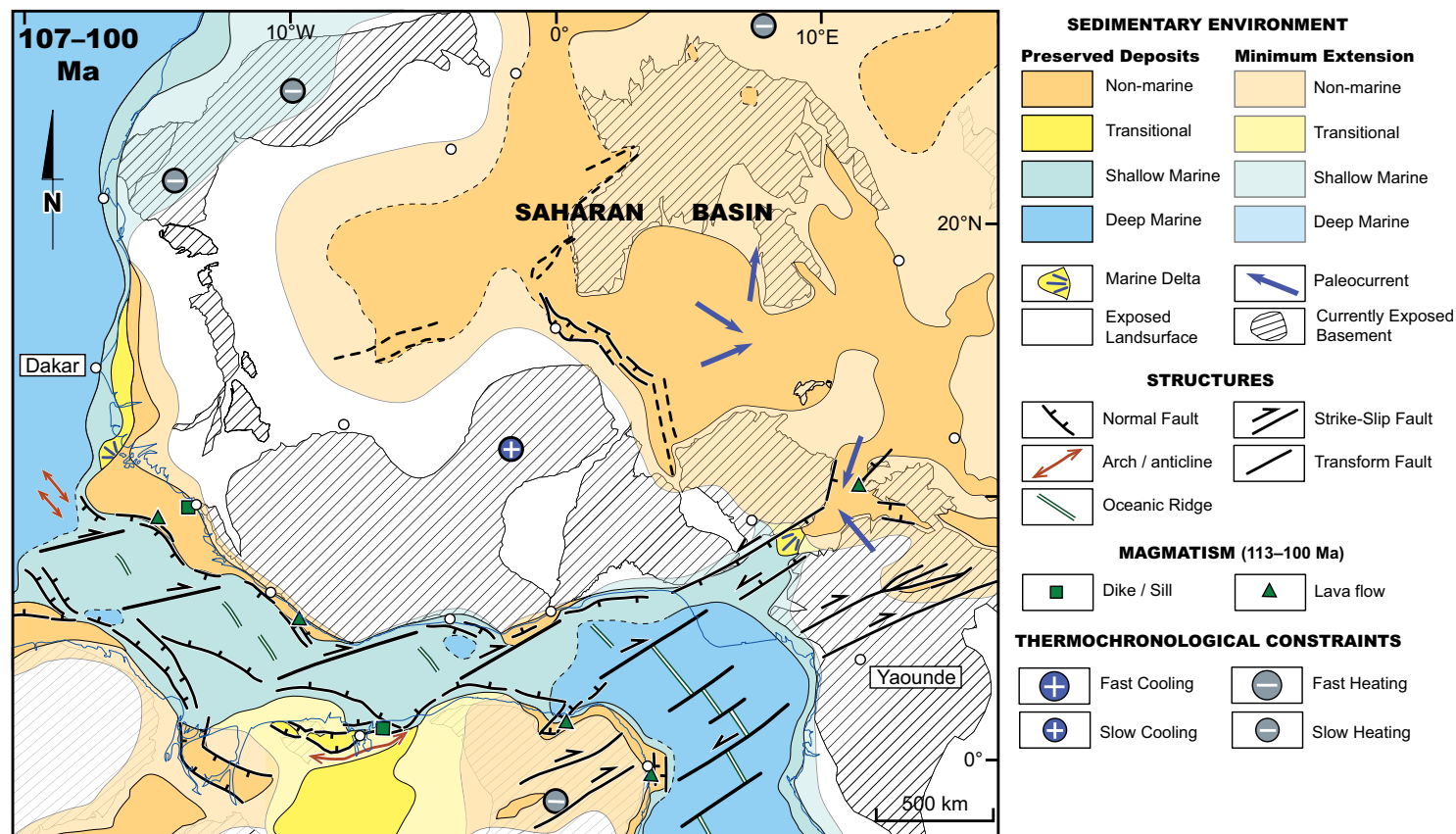


Figure 8. Geological configuration of northwestern Africa, adjoining South America, and the eastern Central Atlantic Ocean during the late Albian (107–100 Ma). Same conventions as in Figure 5.

(see also Fig. 4B) and along the edges of intracratonic basins on the slopes of intracratonic basement highs.

The cross sections show that the preservation of sediments in intracratonic basins is controlled by an interference between intracontinental basement highs and marginal upwarps. Moreover, the growth of the adjoining basement highs would better explain the subsidence histories of these intracratonic basins (Sahagian, 1993). Meso-Cenozoic basins display uneven spatial relationships with preserved Neoproterozoic and Paleozoic depocenters. This suggests a migration of depocenters through time driven by the interference of vertical movement of basement highs and marginal upwarps. The present-day wavelength of the marginal upwarp-intracratonic basin paired systems ranges from 1400 to 2400 km for the equatorial marginal upwarp (Figs. 3B and 3C) to 2400–3200 km

for the Central Atlantic marginal upwarp (Figs. 3A and 3B). On the cross sections, this pattern is disturbed toward the cratonic interior by the Hoggar or Reguibat basement highs, which have typical wavelengths of 700–900 km.

The cross-sectional wavelength of upwarp-marginal basin paired systems goes from 1000 to 1200 km for the equatorial domain to 1200–1600 km for the Central Atlantic domain. Those differences in wavelength are consistent with the width of the pre-rift (i.e., pre-Mesozoic) geological substrate exposed by the marginal upwarps, of 400–800 km for the equatorial domain and 800–900 km for the Central Atlantic domain. This difference may be explained by the age difference between the two margins (with a wavelength increasing along with thermal relaxation and stiffening of the lithosphere through time). Alternatively, the fact that the equatorial margin is mostly transform controlled, and

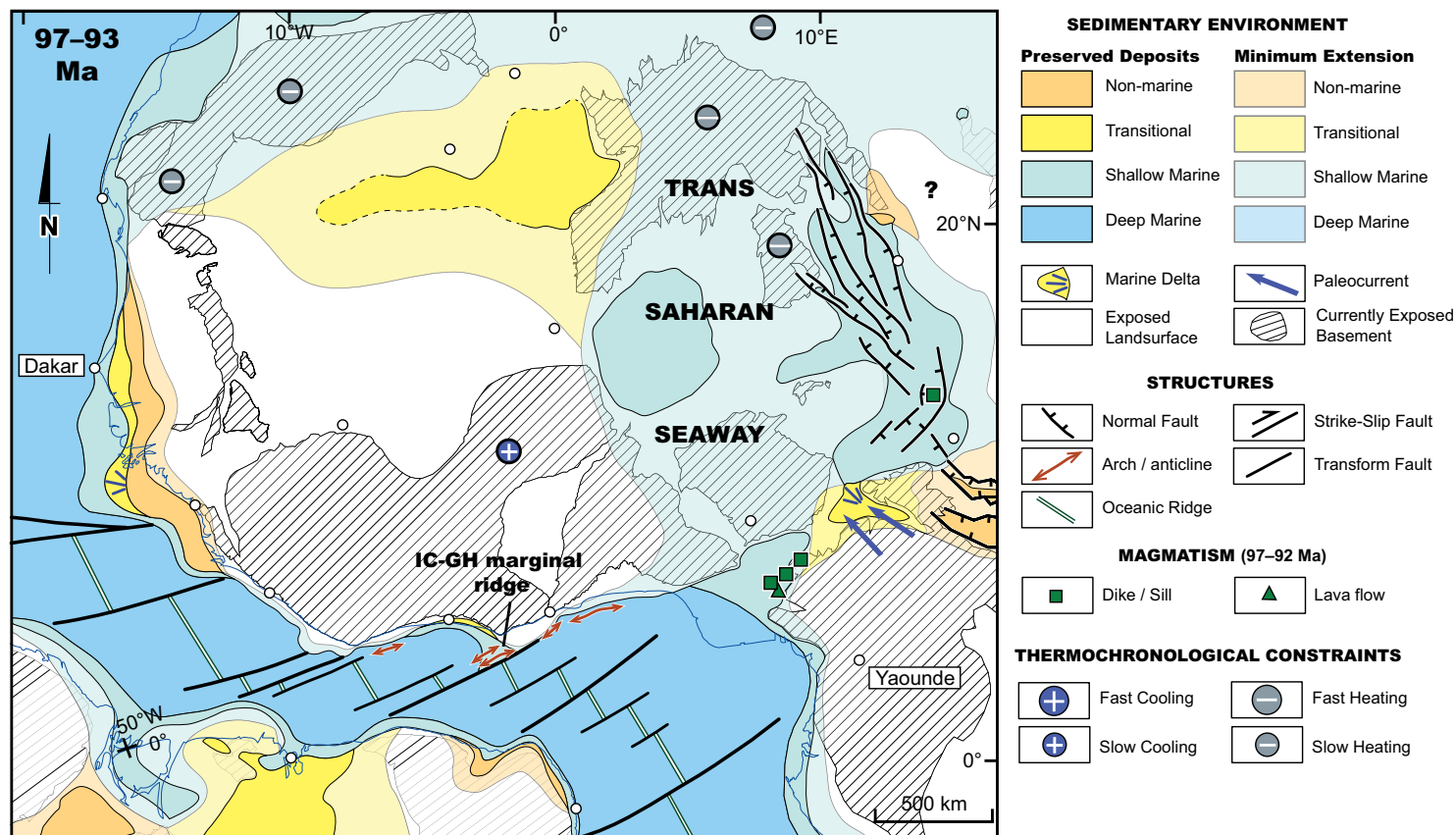


Figure 9. Geological configuration of northwestern Africa, northern South America, and the equatorial and eastern Central Atlantic Ocean during the late Cenomanian (97-93 Ma). Same conventions as in Figure 5.

therefore narrower, would also explain its shorter wavelength with respect to that of the Central Atlantic margin.

Meso-Cenozoic series are thinner in the intracratonic basins (less than 2 km thick) than in the marginal basins (up to 5 km thick). Triassic and Jurassic sediments are mainly preserved along the Central Atlantic margin due to Late Triassic rifting along that margin (Figs. 3A and 3B). Lower Cretaceous postrift deposits are much thicker along the Central Atlantic margin than along the equatorial margin (Figs. 3C and 3D). Cenozoic sediments are thinner but cover wider areas on the Central Atlantic margin, suggesting comparable volumes on both margins. Cenozoic sediments are well preserved along the equatorial Atlantic margin (up to 3 km thick), especially along its Ghana-Benin segment, which has been partly fed by the Niger Delta located farther east (e.g., Fig. 1B).

Paleomaps

Early Jurassic (235-190 Ma): The Central Atlantic Magmatic Province (CAMP) and the Opening of the Central Atlantic Ocean (Figure 5)

During the Early Jurassic, multiple rifts form from north to south along the future Central Atlantic margins and inland northwestern Africa and northern South America (e.g., Labails et al., 2010). Nonmarine sediments and salt deposits accumulate in these rift basins (Olsen, 1997; Brownfield and Charpentier, 2003; Davison, 2005). The extent of these deposits may have been much wider originally, given the pervasive unconformity truncating the late synrift sediments (Olsen, 1997; Withjack et al., 1998). The Guinea-Liberia margin segment

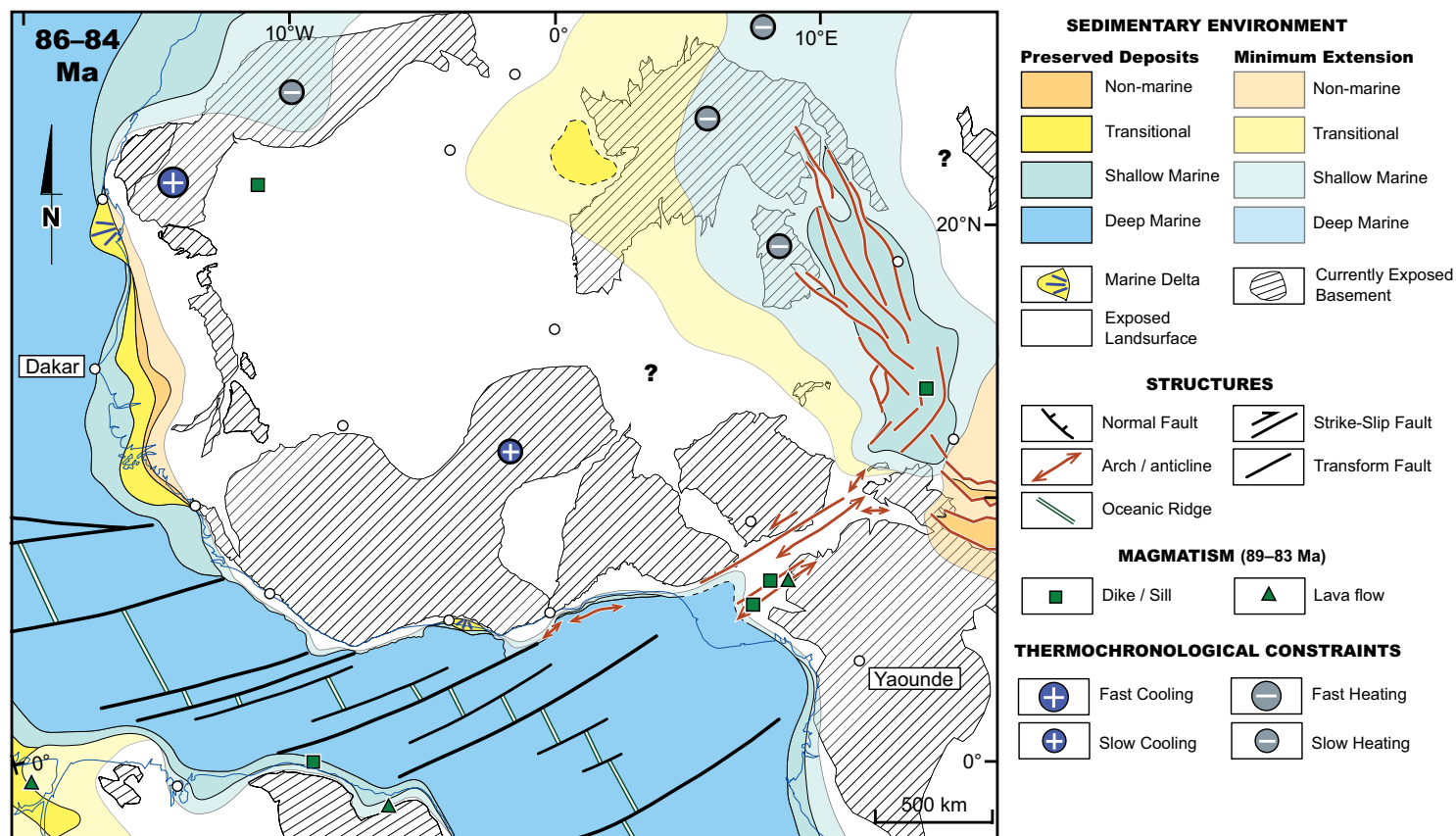


Figure 10. Geological configuration of northwestern Africa, northern South America, and the equatorial and eastern Central Atlantic Ocean during the Santonian (86–84 Ma). Same conventions as in Figure 5. Faults undergoing inversion are shown in red.

seems to experience crustal stretching at this time, given the accumulations of aeolian sediments interbedded with basaltic lava flows reported in South America (Figueiredo et al., 2007; Soares Júnior et al., 2011). This, together with our observations on unpublished seismic lines, suggests the occurrence of a Central Atlantic rift branch along the future Guinea-Liberia margin segment of the equatorial Atlantic. This rift may then have been activated during rifting of the equatorial Atlantic domain (see below). On the continent, nonmarine sediments (mainly siltstones) are deposited in the northeasternmost part of the study area, with paleocurrents to the N or NW (Valsardieu, 1971; Genik, 1993). The Central Atlantic Magmatic Province (CAMP, dated at 235–185 Ma with a peak activity at 200 Ma; Jourdan et al., 2009; Table S2 in Supplemental File 1 [see footnote 1]) affects most of the exposed domain in the form of lava flows, sills, and dikes. Large sills may still be buried within the Taoudeni basin, as well

as onshore South American basins. Outside the CAMP, ring complexes were emplaced in the Nigeria shield (the “Younger Granites,” dated at 213–141 Ma) and near the Hoggar shield (dated at 215–166 Ma). Most of the northwestern African continental domain outside the Central Atlantic rift system may have been subjected to erosion, possibly forming a “CAMP superswell” drained by a river system feeding a proto-Saharan basin.

Valanginian (140–133 Ma): Pre-Rift Configuration (Figure 6)

Because seafloor spreading has been taking place since the Early Jurassic, the Central Atlantic domain of Africa has long reached its postrift stage and still builds a continental shelf during the Valanginian (Dillon et al., 1988;

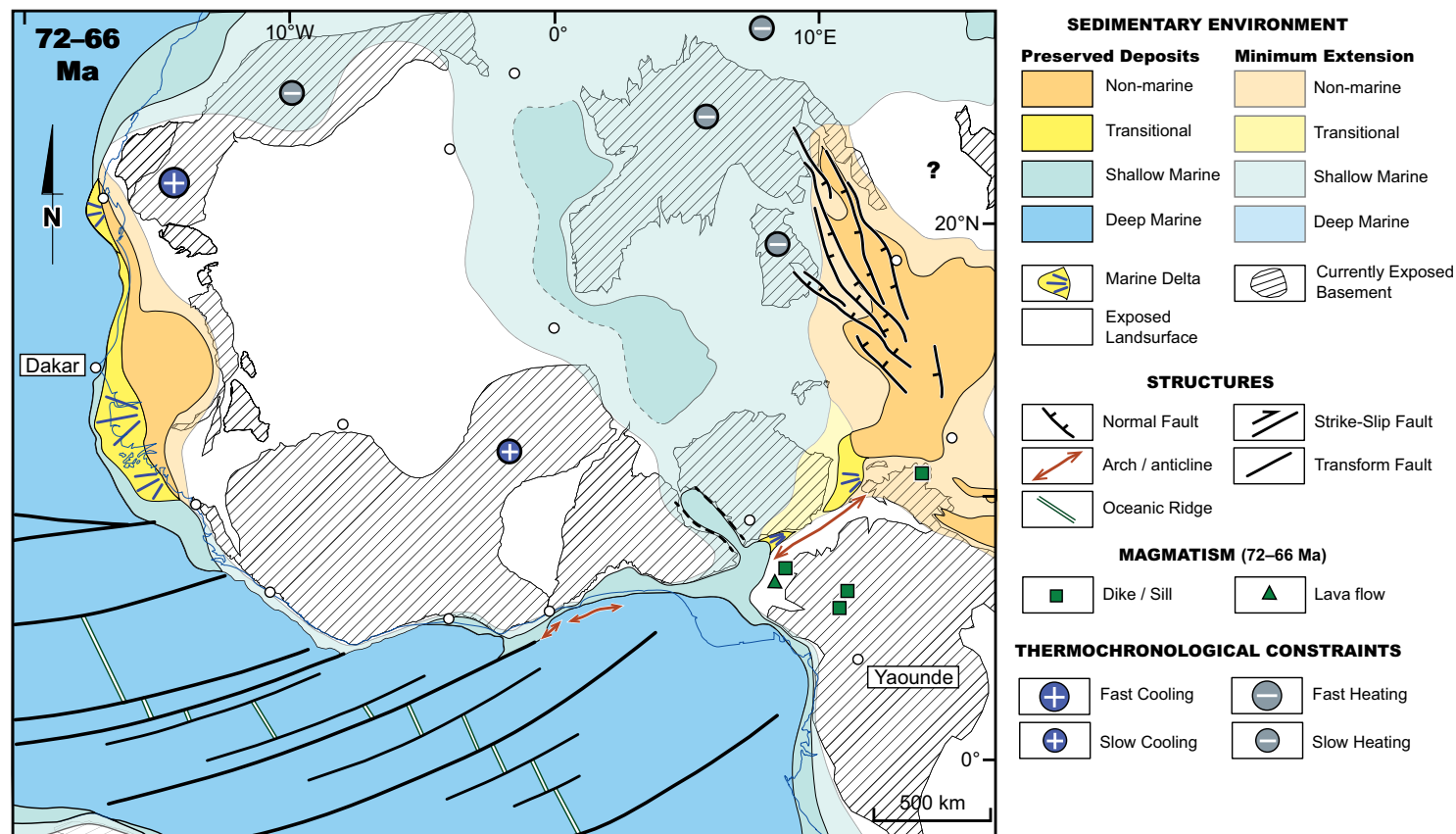


Figure 11. Geological configuration of northwestern Africa and the equatorial and eastern Central Atlantic Ocean during the Maastrichtian (72–66 Ma). Same conventions as in Figure 5.

Davison, 2005; Baby et al., 2014). Rifting takes place along the future Guinea Plateau (Fig. 2) and its South American counterpart (the Demerara plateau), where Valanginian synrift sediments have been reported by Gouyet (1988). In this domain, the oldest synrift sediments have been reported as probably Neocomian (Berriasian to Hauterivian) by Figueiredo et al. (2007) and Zalán and Matsuda (2007). The corner shape extensional domain near the southeasternmost Central Atlantic Ocean is prolonged to the SE by two potential NW-trending rifts, suggesting southeastward propagation of the rift system. The first of these two rifts initiated along the future Sierra Leone–Liberia margin segment, potentially reactivating the structures formed during the Central Atlantic rifting (Fig. 5). The second rift formed within northern South America (Cassipore and Marajo graben; Figueiredo et al., 2007; Zalán and Matsuda, 2007). The NE-trending Tacutu rift continues to be filled with continental sediments after its initiation in the Late Jurassic (Vaz et al., 2007b). The future South Atlantic

domain consists in a wide rift system preserving nonmarine sediments (de Matos, 1992; Chaboureau et al., 2013). It is mostly located in intracontinental South America and interacts with ENE-trending transfer faults (future transform faults) reactivating Pan-African shear zones (e.g., Popoff, 1988).

In intracontinental Africa, a large alluvial basin (named hereafter the Saharan basin) developed. It is separated from the margins of the Central and future equatorial Atlantic margins by a wide erosional domain. Thermochronological data (Gunnell, 2003; Leprêtre, 2015; Leprêtre et al., 2015) as well as widespread kimberlitic magmatism are consistent with uplift in this domain. According to paleocurrent data, erosion of the upwarp fed the Saharan basin, which is, at the time, connected to the Tethys Ocean farther north (Guiraud et al., 2005). Magmatic activity is widespread over northern South America since the Latest Jurassic, inside and mostly outside the rifts. River systems crossing the future equatorial Atlantic domain may not be precluded at the time.

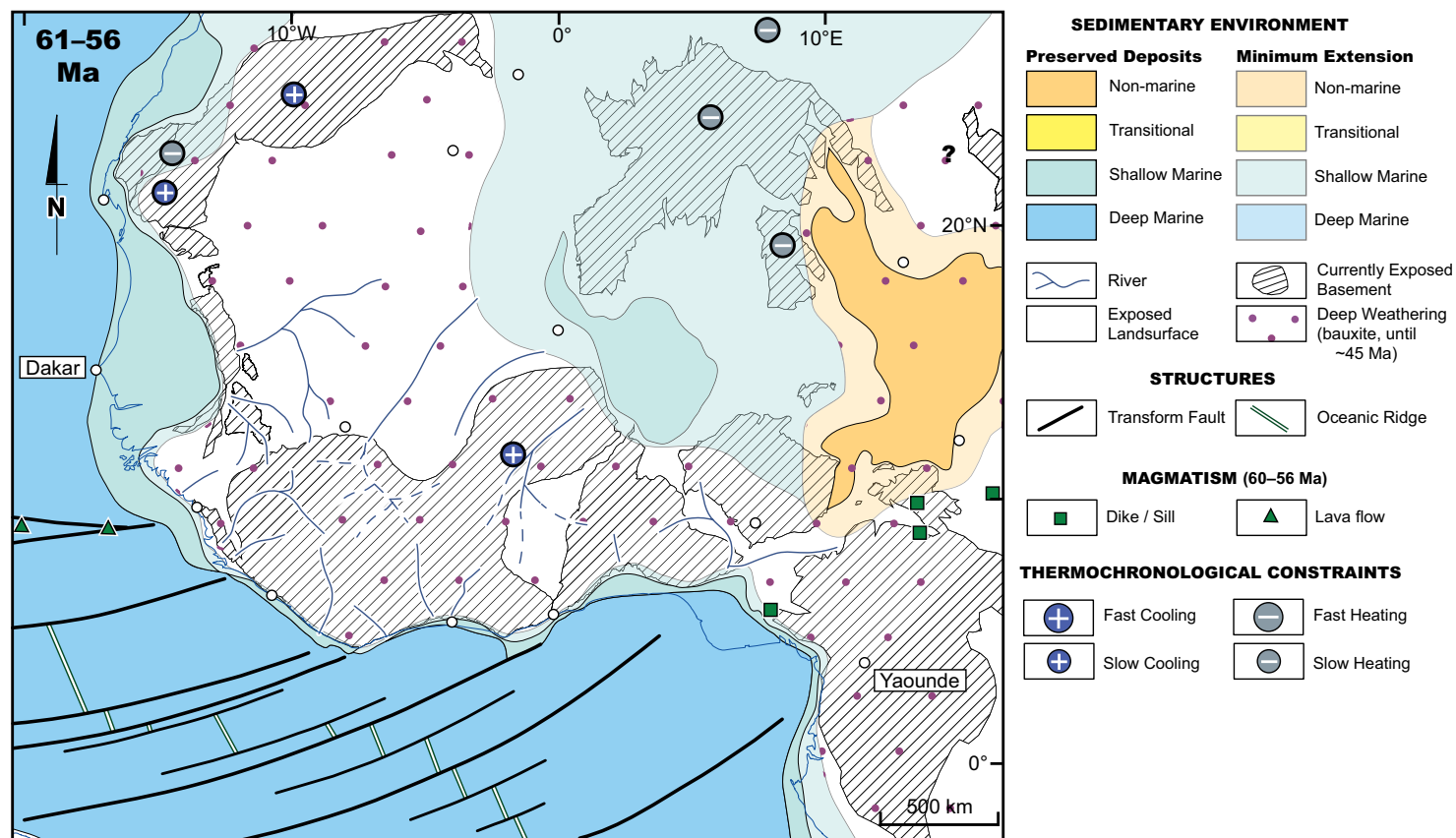


Figure 12. Geological configuration of northwestern Africa and the equatorial and eastern Central Atlantic Ocean during the Late Paleocene (61–56 Ma). Same conventions as in Figure 5.

Middle Aptian (120–115): Main Rift Phase (Figure 7)

By middle Aptian, rifting affects the entire equatorial domain with ENE-trending, dextral strike-slip faults (future transforms) and NW- to W-trending normal faults, forming an en echelon rift system. Mafic lava flows emplace in this rift system, as well as over intracontinental South America. If seawater may have invaded the Guinea-Liberia margin segment from the NW, the Ivory-Ghana and Ghana-Benin marginal basins remain under fluvial-lacustrine sedimentation environment. In the Saharan basin, the Western and Central rift system and the Gao rift are active and receive Barremian (?) to Albian continental clastic sediments (Fig. 1). A nonmarine alluvial plain occupies the future Benue Trough, connecting the Saharan basin to the equatorial rift basins. Paleocurrents indicate that this alluvial plain is at least partly fed from the NE, suggesting tapping of sediments from the Saharan basin.

A 300–1500-km-wide erosional upwarp separates the Saharan basin from the Central Atlantic margin and the equatorial rift system, probably feeding those basins with clastic sediments. Aptian sediments filling up the equatorial rift system may also come from the denudation of the exposed South American continental surface.

Large-scale transpressional inversion structures (E-W folds and oblique-reverse faults shown in red on the map) affect the southern margin of the Guinea plateau (Benkheilil et al., 1995) and that of its South American counterpart (the Demerara plateau; Gouyet, 1988; Sapin et al., 2016; Fig. 7). This inversion takes place in the vicinity of the future Guinea fracture zone that separated the two plateaus, at the junction between the Central and future equatorial Atlantic Oceans. Shortening also affects intracontinental South America, forming several EW- and NS-trending arches along sedimentary basin margins (de Almeida et al., 1981; Soares Júnior et al., 2008). Middle Aptian inversion

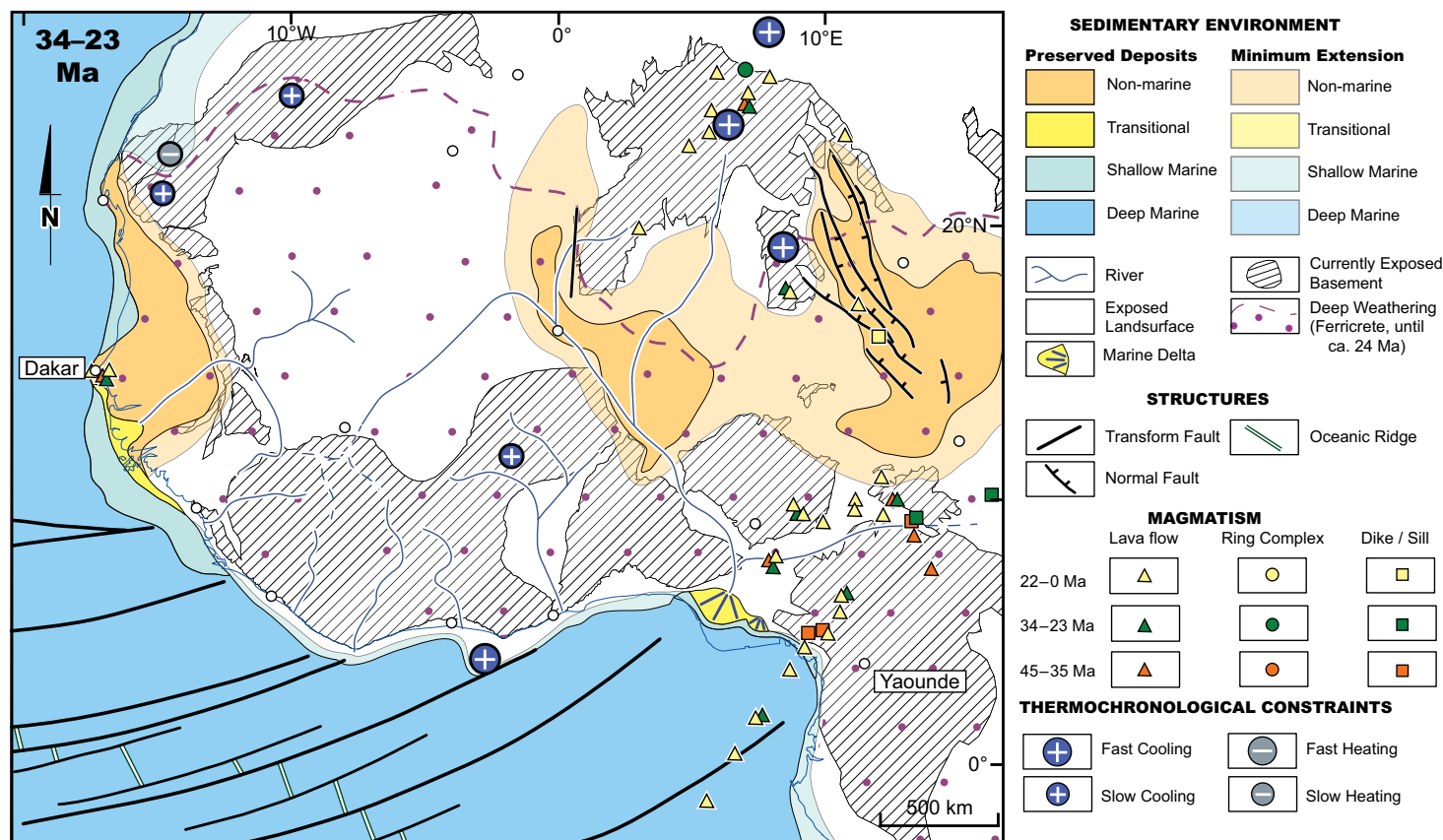


Figure 13. Geological configuration of northwestern Africa and the equatorial and eastern Central Atlantic Ocean during the Oligocene (34–23 Ma). Same conventions as in Figure 5.

along the future Guinea transform was interpreted by Benkheilil et al. (1995) as an adjustment in plate kinematics. This inversion event is recorded on a very large scale all along the Central Atlantic margins (so-called “Austrian phase”). We tentatively suggest that a jump to the south in the rotation pole of Africa can explain inversion at the southern tip of the Central Atlantic domain as the equatorial rift system started to open east of the future Guinea-Liberia margin segment. This kinematic adjustment could explain the abandonment of the rift system that previously propagated along NW-trending structures into the South American continent (Fig. 6). This mid-Aptian inversion has had a major impact on the structure of the northwesternmost equatorial oceanic lithosphere of the African plate. Indeed, N-S shortening has induced the eastward converging pattern of the transforms against the Guinea fracture zone as seen on the geologic map of the world (Bouysse, 2014; see also figure 2 in Moulin et al., 2009).

Late Albian (107–100 Ma): Lithospheric Breakup and Onset of Seafloor Spreading (Figure 8)

In the late Albian, new WNW-trending rifts form along the South American margin between the Romanche and the Saint Paul fracture zones (Soares Júnior et al., 2008, 2011). The main normal faults of the equatorial rift system remain active. Inversion continues to affect the African margin at the junction between the Central Atlantic and equatorial domains. Magmatism is reported locally along the equatorial Atlantic margins. Intracontinental African rifts ceased their activity (except the Gao rift), and a corridor of shallow-marine anoxic seawater invades the narrow equatorial Atlantic Oceans, connecting the Central and South Atlantic Ocean (at ca. 104 Ma; MacGregor et al., 2003; Brownfield and Charpentier, 2006). Strike-slip and normal faulting along the equatorial margins ends during the late Albian, as shown by an ubiquitous

breakup unconformity. The Ivory Coast–Ghana marginal ridge (offshore Accra, Fig. 2) is considered as the last connection between the two continents before the ultimate breakup, which leads to seafloor spreading along the whole equatorial domain. The Saharan alluvial basin is still functional and drained northward and westward (Valsardieu, 1971). Sinistral transtensional faulting is documented in the Benue Trough (Benkhelil, 1988; Benkhelil et al., 1998). A marine delta forms in the middle of the Trough, connecting the Sahara basin to the equatorial Atlantic Ocean. This delta appears to be fed from the southernmost Saharan basin and by the South Atlantic marginal upwarp of Africa. A coastal plain develops in a very large embayment on South America, attesting to very low regional continental topography and slopes. The surface of exposed land has not evolved significantly since the Aptian in northwestern Africa. The African marginal upwarp feeds both the Saharan basin and the Atlantic margins. From this time on, no river systems will connect Africa to South America.

Late Cenomanian (97–93 Ma): Maximum Continental Flooding (Figure 9)

The global maximum transgression during the late Cenomanian–early Turonian flooded the Saharan basin. A “trans-Saharan seaway” connected the Tethys Ocean, in the north, to the equatorial Atlantic Ocean, in the south (Reyment, 1980; Luger, 2003), and shallow-marine brackish shales and limestones were deposited (Dufaure et al., 1984; Zanguina et al., 1998). Thermochronological data suggest burial of the Hoggar and Reguibat shields (Rougier et al., 2013; Leprêtre et al., 2014, 2015; English et al., 2016), consistently with subsidence under the “trans-Saharan seaway” and the northwestern Sahara basin. A wide lagoonal domain formed between these two domains, which underwent alternating transgressions and regressions (Fabre et al., 1996). In addition, marine flooding of the Sahara in the Late Cretaceous (this also applies to the next two considered periods, i.e., Santonian and Maastrichtian; Figs. 10 and 11) consisted of episodic transgressions and regressions over a wide and very low-relief and low-topography surface rather than of long-lasting drowning (Rat et al., 1991). Enhanced shoreline mobility during those periods must have led to transient and limited erosions.

The Upper Benue Trough still receives deltaic sediments mostly provided by the South Atlantic marginal upwarp. A late Cenomanian–Turonian marine transgression is recorded along the Central and equatorial Atlantic margins without significant inland shoreline migration (Brownfield and Charpentier, 2003; Baby et al., 2014). This transgression is documented farther inland in South America in at least two embayments, suggesting the persistence of a very low topography on that side of the equatorial Atlantic Ocean. Transform faults are still active as the mid-ocean ridges migrate along the Ivory Coast–Ghana marginal ridge, i.e., the “active transform margin” stage of Basile et al. (2005). Anticlines form at the African tip of the Romanche and Saint Paul transform faults as a result of transpression. The equatorial Atlantic Ocean seems to undergo restricted bottom-water circulation as attested to by sedimentological and paleontological evidence (black shales and Oligosteginid limestones; Dumestre and Carvalho, 1985; Chierici, 1996; Brownfield and Charpentier, 2006).

In Africa, the area exposed to erosion does not change significantly. The marginal upwarp is flooded north of 20°N, whereas a wider surface corresponding to the Man-Leo Shield and the southern Taoudeni basin undergoes erosion. The South Atlantic marginal upwarp feeds both the trans-Saharan seaway and the easternmost equatorial margin of Africa through the Benue delta. The occurrence of a continental alluvial plain east of the Benue delta could suggest the occurrence of a river system large enough to provide sediments from Central or East Africa to the delta.

Santonian (86–84 Ma): Regional Tectonic Inversion (Figure 10)

During the Santonian, sinistral transpression leads to the inversion of the Benue Trough, producing regional folds and schistositicities and forming a mountain range that recorded ~12 km of shortening (Benkhelil and Guiraud, 1980; Benkhelil, 1987, 1988; Benkhelil et al., 1988). The shortening direction varies from N to NW. Transpressional structures are also documented in the Western and Central rift system (Guiraud and Bosworth, 1997) associated with shallow-marine sediments deposited during inversion. A narrow seaway of the Tethys floods the Western and Central rift system. This seaway is probably bounded by lagoonal environments to the west (Fabre et al., 1996). Thermochronological data suggest that the Hoggar shield remains buried at the time.

Seismic stratigraphy of the equatorial Atlantic margins argues for more than 200 m of relative sea-level fall during the considered time interval (this work). Considering the fact that the period corresponds to a long-term high eustatic level, the locally observed base-level fall may only be explained by an uplift of the margin. The Santonian sedimentary hiatus documented along the Sierra Leone–Liberia margin segment also indicates uplift and erosion at that time. Furthermore, vitrinite reflectance data from boreholes along the equatorial Atlantic margin indicate at least 400–500 m of erosion during the Late Cretaceous, which may be related to that same event. Transform-controlled anticlines continue to grow along the Ghana-Benin margin segment. Reactivation of the Romanche transform fault leads to over 1 km of erosion on the Ivory Coast–Ghana marginal ridge (Figs. 1 and 9) during the Late Cretaceous (unpublished vitrinite reflectance data). In northwestern Africa, the area exposed to erosion has grown significantly, suggesting a very long wavelength uplift that could be, partially or totally, related to the inversion event. This eroding domain is very wide and continuous, from the South Atlantic margin to the Reguibat shield.

Maastrichtian (72–66 Ma): Brief Continental Flooding and Re-Establishment of the Trans-Saharan Seaway (Figure 11)

During the Maastrichtian, a marine transgression also briefly flooded West Africa. Marine sediments interbedded within brackish-water deposits are preserved east of the subsiding Hoggar shield. The trans-Saharan seaway is nonetheless probably re-established, as suggested by the faunal similarities between the equatorial Atlantic Ocean and the trans-Saharan seaway (Reyment, 1980; Luger, 2003). It is likely that the connection is made through the

Bida rift, which began to form in the Campanian and continues to develop during the Maastrichtian under shallow-marine environment (Kogbe et al., 1983; Akande et al., 2005; Ojo and Akande, 2009). Transgression is also recorded on the Ivory Coast–Ghana and Ghana-Benin margin segments by the flooding of the coastal basins.

The Western and Central rift system is reactivated in extension and accommodates the deposition of alluvial sandstones (Zanguina et al., 1998). Overfeeding of the rifts may explain the change from marine to continental depositional environments, even though more accommodation space is created by fault reactivation. The eastern shoreline of the trans-Saharan seaway was most likely mobile during the considered period and may have been associated with transient erosion at the Hoggar and Nigerian shield areas.

Folding is probably still active in the Upper Benue Trough, resulting in a Maastrichtian unconformity (Benkhelil, 1982). Reactivation of folding at the African tip of the Romanche transform fault is also documented. Regional deformation seems to result from W- to WNW-directed extension (and potentially shortening normal to that direction). Magmatism only affects the Lower Benue Trough and the adjoining Cameroun Line (Fig. 1B). Transgression leads to a slight reduction of the erosional area, by flooding of the Nigerian shield area and part of the Saharan domain. The installation of large deltaic systems along the Central Atlantic coast could suggest drainage reorganization and/or upwarping of that margin. The Western and Central rift system could still be fed by distant source areas to the east of Chad Basin.

Late Paleocene (61–56 Ma): Last Flooding and Intense Continental Weathering (Figure 12)

A last transgression affected northwestern Africa during the Paleocene, and inland shoreline migration has been documented along the Central and equatorial Atlantic margins. Marine limestones and shales were deposited in the coastal basins (Davison, 2005; Brownfield and Charpentier, 2006), as well as in the Saharan basin, recording southward transgression of the Tethys onto the location of the former trans-Saharan seaway, although without reaching the equatorial Atlantic Ocean. Extension in the Western and Central rift system stopped, and Chad Basin underwent long-wavelength subsidence and was filled by fluvial sediments. Shoreline migration and potential associated erosion may still take place on the western margin of the Chad alluvial plain system.

No major faulting is documented over the study area. Intense weathering is favored by peak greenhouse climate, allowing bauxites to develop all emerged lands (Beauvais and Chardon, 2013; Chardon et al., 2016). The preservation of bauxites over the Nigerian shield and the Bida rift (Valeton, 1991) precludes the connection between the equatorial Atlantic Ocean and the Tethys (Chardon et al., 2016). Because continental chemical weathering is favored, correlative carbonates and phosphates are found in all West African basins, and clastic fluxes through the river systems are subdued (e.g., Lang et al., 1990; Valeton, 1991; Johnson et al., 2000). The size of the erosional domain did not evolve significantly and a continuous marginal upwarp was re-installed.

Oligocene (34–23 Ma): Development of Basin-and-Swell Topography (Figure 13)

Volcanism developed on the African plate from the Late Eocene onward at various locations outside the West African craton. On the Hoggar shield and along the Cameroon line, the volcanism is interpreted as “hotspot” related (Ait-Hamou and Dautria, 1994; Liégeois et al., 2005; Ait-Hamou, 2006; Ngako et al., 2006; Table S2 in Supplemental Item 1 [see footnote 1]). Temperature-time paths of apatites suggest that the Hoggar shield underwent exhumation since the Late Eocene (40–30 Ma; Rougier et al., 2013; English et al., 2016). The products of its erosion are emplaced as mega fans of the “Continental Terminal” around the uplifting massif (Chardon et al., 2016). Doming of the Hoggar shield led to the individualization of the present-day intracontinental basins of northwestern Africa by fragmentation of a single large Saharan basin into the Taoudeni, South Algerian, Murzuq, Chad, and Iullemeden basins. This fragmentation contributed to the development of the “basin-and-swell” topography of the continent (Burke, 1996). This also triggered definitive retreat of the sea from the continent and a major drainage reorganization, which led to the establishment of the modern river network during the Early Oligocene, allowing, in particular, for the building of the Niger delta (Chardon et al., 2016). Numerous canyons incised the shelf and slopes of the equatorial and South Atlantic margins of Africa, starting in the late Early Oligocene (Simon and Amakou, 1984; Burke, 1996; Seranne and Nze Abeigne, 1999; this study). This major unconformity may be tentatively linked to continental-scale uplift accompanying the development of the basin-and-swell topography (Burke et al., 2003). Some authors suggest that the Western and Central rift system reactivated in the Eocene–Early Oligocene, allowing for the deposition of fluvial-lacustrine sediments (Genik, 1992, 1993; Zanguina et al., 1998). A phase of lateralization affected the entire subregion until Latest Oligocene (Chardon et al., 2016). No sediment accumulated on the continent from that time on, except in the Chad Basin, which continued to subside during the Neogene (Burke, 1976).

■ DISCUSSION

Rifting and Large-Scale Kinematics

Our reconstruction of the rifting stage (120–115 Ma; Fig. 7) shows that the network formed by the equatorial rift system and the intracontinental African rifts subdivided the continent areas into seven microplates (Fig. 14). This configuration allowed for refining the kinematic framework for Early Cretaceous rifting, which is usually based on a four-microplate model (South America, NW Africa or Western block, Arabian-Nubian block, and South Africa or austral block; Guiraud and Maurin, 1992; Maurin and Guiraud, 1993). In the present work, microplates are defined as continental domains without detectable faulting or continuous deformation, which are bounded by corridors of tectonic structures (rifts and transcurrent faults) active during the main rift phase (Figs.

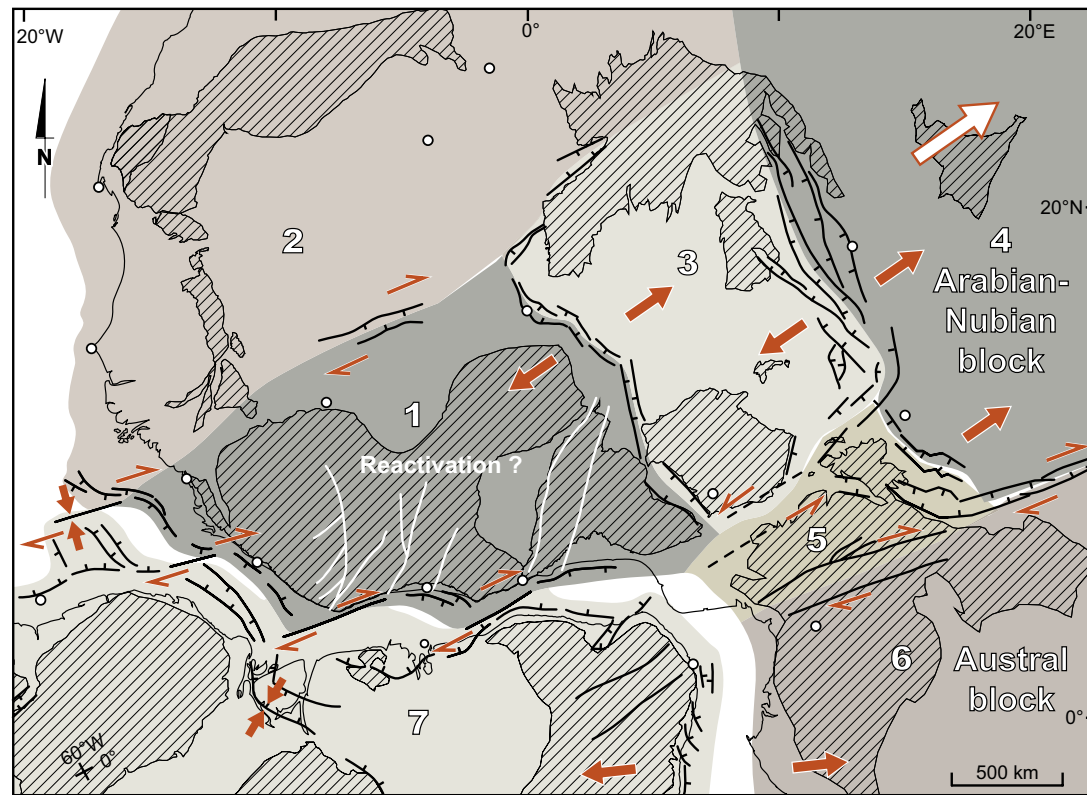


Figure 14. Microplate model for northwestern Africa and adjoining northern South America during Aptian rifting (the model corresponds to the reconstruction shown in Fig. 7, at 115 Ma). Six microplates are distinguished in intracontinental Africa. Open circles are the localities from Figures 1 and 2B.

7 and 14). Those blocks, with the exception of South America (microplate 7), remained apparently undeformed during the entire Meso-Cenozoic.

A central microplate 1 (Leo-Man and Nigerian shields) is bounded to the south by the en echelon equatorial rift system and to the NE by the Gao-Bida rift system (Figs. 1B and 14). Its northwestern limit is a transfer fault system, which includes the Nara and Amded rifts (Fig. 14). This fault system may be seen as an intracontinental extension of the Guinea-Demerara plateaus bounding fault (i.e., the future Guinea transform), which will mark the boundary between the Central and the equatorial Atlantic domains. To the north, microplate 2 represents the African continental lithosphere of Central Atlantic affinity. Microplate 3 accommodates NE-directed extension between microplate 1 and the Arabian-Nubian plate (microplate 4) drifting northeastward (Fig. 14). Microplate 5 (Benue block) occupies an intermediate position between microplates 1, 3, 4, 6 (Austral block), and 7, and has therefore a complex behavior given the kinematic incompatibilities it must absorb along its various boundaries. Nevertheless, microtectonic data that support sinistral and dextral slip along its northern and southern boundaries, respectively (Benkheilil, 1988),

could suggest escape of that block toward the ENE, in the direction of relative displacement of the Arabian-Nubian block (microplate 4; Fig. 14).

Our study also shows that the rifting history of the equatorial Atlantic domain does not result from a simple combination of coeval dextral strike-slip and normal faulting at the scale of the whole margins (Fig. 15). The Ivory Coast-Ghana and Ghana-Benin margin segments were rifted during the Barremian-Albian. The Guinea-Liberia margin segment was rifted earlier because it formed in a weakness zone corresponding to an earlier Jurassic rift (or aulacogen) of the Central Atlantic Ocean (Figs. 5 and 15A). The South American rift pattern is more complex than its African counterpart. This is due to the early propagation of a Guinea-Liberia rift system into South America (Fig. 15A) and to the presence of the Sao Luis craton (Klein and Moura, 2008) that acted as a rheological lithospheric heterogeneity (Fig. 15B). Mantle exhumation and/or seafloor spreading initiated at an early time in isolated patches even if rifting remained active (Figs. 8 and 15B). Those newly formed isolated "ocean basins" evolved under restricted water circulation during the Albian-Cenomanian, as attested to by foraminiferal

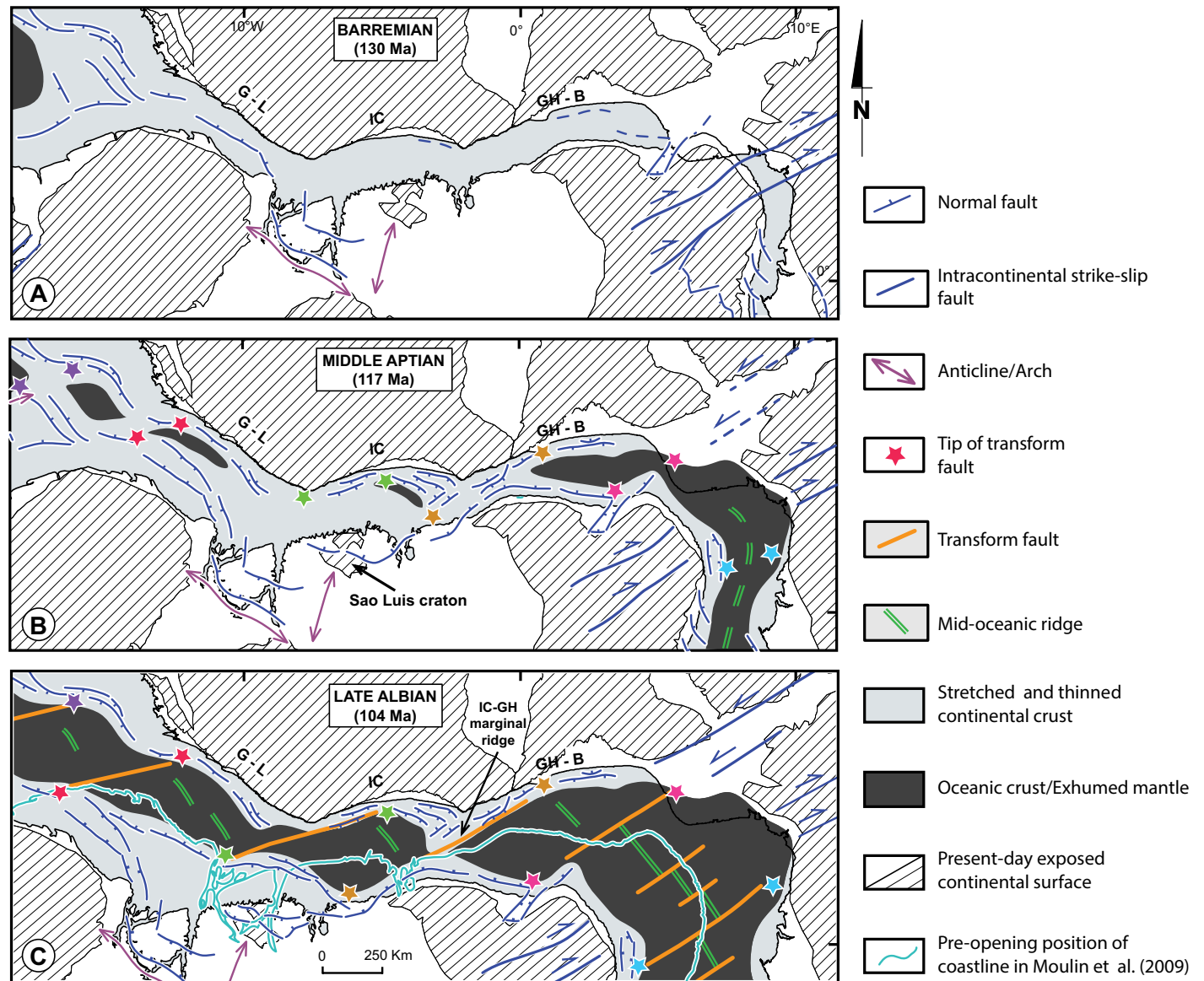


Figure 15. Successive configurations of the equatorial Atlantic Ocean during the Early Cretaceous. G-L—Guinea-Liberia margin segment; IC—Ivory Coast margin segment; GH-B—Ghana-Benin margin segment. (A) Barremian (130 Ma): the Guinea-Liberia margin segment was undergoing rifting, whereas rifting only initiated along the Ivory Coast and Ghana-Benin margin segments. (B) Main Aptian rifting stage (117 Ma): the equatorial Atlantic margins underwent interference between dextral strike-slip (along incipient transforms) and normal faulting. Oceanic spreading was active between the South Atlantic Ocean and the eastern half of the Ghana-Benin margin segment. Spreading also initiated along the Ivory Coast–Ghana and Guinea-Liberia margin segments, forming two isolated domains of oceanic crust. (C) Late Albian breakup stage (104 Ma). A WNW-trending rift branch formed during the earlier stage on the South American side and was still active at the time. Rifting then ceased, and ultimate breakup took place along the Ivory Coast–Ghana marginal ridge.

communities typical of euxinic conditions and the absence of benthic foraminifera, as well as the occurrence of black shales indicative of reducing environments. Restriction of water circulation may be interpreted to result from the potential barrier effect of the transform-related marginal ridges (Figs.10 and 15C). The African equatorial margin acquired its segmentation only after final continental breakup in the late Albian (Fig. 15C), which took place along the Ivory Coast–Ghana marginal ridge (Fig. 15C). Our new synrift fault map pattern requires the integration of a wide zone of synrift continental deformation to reconstruct a pre-opening fit between Africa and South America (Fig. 15C). Our fit is significantly different from that based on the correlation of magnetic lineaments and transforms across the equatorial Atlantic Ocean (Moulin et al., 2009), which implies a much narrower (of up to 300 km) gap between the two continents (Fig. 15C).

Long-Wavelength Deformation, Marginal Upwarps, and Sedimentary Basins

Our work suggests the repeated or sustained occurrence of erosional marginal upwarp(s) between intracratonic and marginal basins around northwestern Africa. Figure 16 shows a stack of the limits (minimum extension) of the sedimentation areas from the Early Jurassic to the Oligocene over intracontinental Africa (compiled from Figs. 5–13). This allows visualizing the evolving shape and size of the maximum erosional areas associated with marginal upwarp(s) through time. Four upwarp segments with contrasted exposure histories may be distinguished (Fig. 16).

The largest and widest upwarp segment (I) coincides roughly with the present-day exposure of the Leo-Man shield. It is 1000 to 1400 km wide and

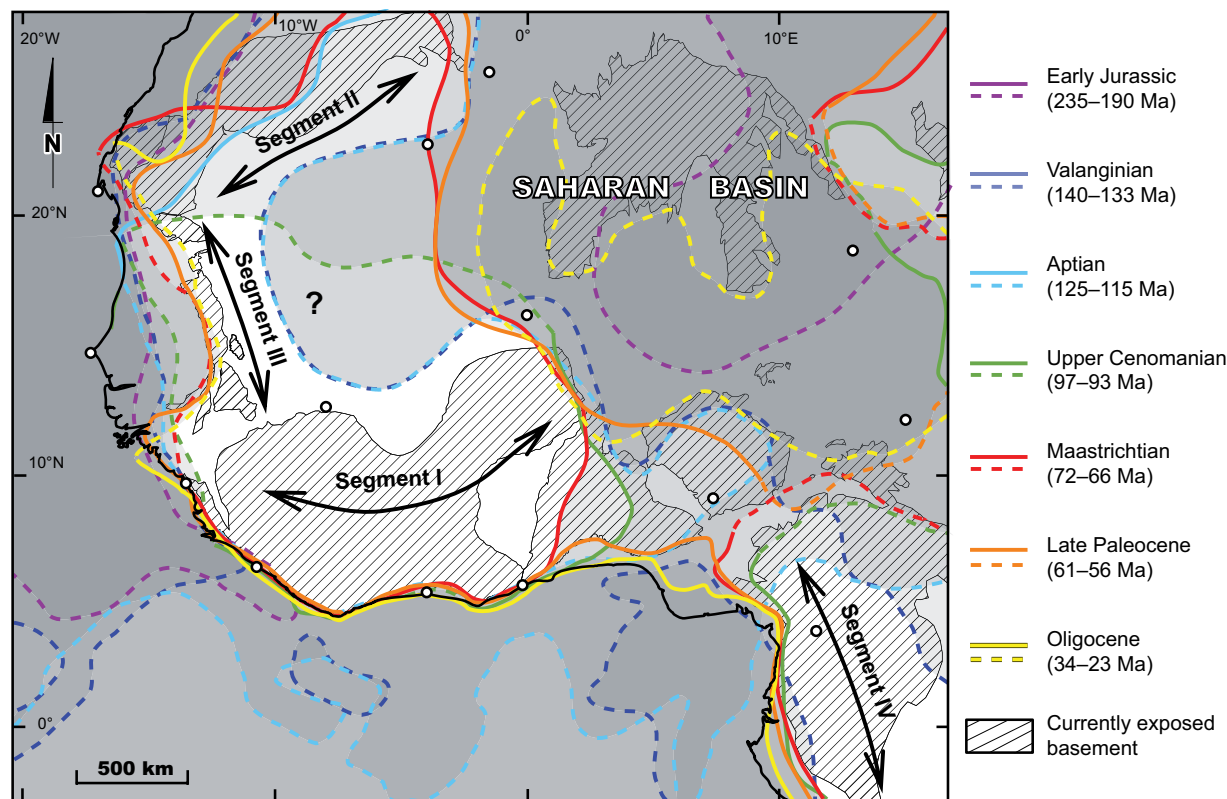


Figure 16. Synthetic paleogeographic map of northwestern Africa showing the evolving positions of shorelines (solid lines) or minimum extent of nonmarine sedimentary deposits (dashed lines) through the Meso-Cenozoic (from Figs. 5–13). Depositional areas are filled with levels of gray. Darker zones represent longer-lived depositional and/or sediment preservation area. Four segments (I to IV) of the marginal upwarp are distinguished on the basis of their exposure and/or flooding histories (see text for further explanation).

may have undergone continuous erosion since the Triassic. The very long wavelength of that upwarp segment (>1500 km) suggests an asthenospheric control and limited influence of the continental margin's evolution, which is expected to produce deformation with much shorter flexure-related wavelengths. All the kimberlites documented in West Africa are located within segment I. Emplacement of the Leo-Man shield kimberlitic province between 150 and 135 Ma (Fig. 6) likely impacted the chemical and physical nature of the lithospheric mantle. This may have provided enough buoyancy for sustaining emersion of that region (see also, for instance, Ault et al., 2015). Upwarp segment II, along the southeastern edge of the Reguibat shield, has a NE trend, is narrower (300–700 km; Fig. 16), and has been flooded at least once. Given its trend parallel to the Reguibat shield, segment II is likely an expression of the vertical movement history of this basement high. Leprêtre (2015) and Leprêtre et al. (2015) suggested that the Reguibat shield underwent repeated upwarping during the Mesozoic in response to plate-boundary forces. Upwarp segment III is north trending (i.e., parallel to the coast) and narrow (400–450 km). It encompasses the Mauritanides mobile belt and the western fringe of the Taoudeni basin (Figs. 2 and 16) and may have been episodically flooded during the Mesozoic. It most likely reflects the long-term evolution of the Senegalese segment of the Central Atlantic margin. The last upwarp segment (IV) relates to the South Atlantic margin. Its considerable width (up to more than 500 km) and the uplift it has undergone during the Neogene (Guillocheau et al., 2015) suggest at least a recent mantle support.

Rouby et al. (2013) have shown that flexure-related rift shoulders of a passive margin are often eroded away 10–20 m.y. after the onset of rifting and therefore cannot explain the persistence of those upwarps for more than 100 m.y. On the other hand, Gilchrist and Summerfield (1990) have shown that denudational flexural isostasy of the seaward slope of upwarps could sustain marginal upwarp topography over long periods. However, flexurally sustained upwarps have wavelengths of a few hundreds of km and cannot explain the >1000 km width of the northwestern African upwarps. To summarize, the documented marginal upwarps are somehow linked to the formation and/or the long-term evolution of the continental margins around northwestern Africa. But their width and/or its evolution through time suggest asthenosphere dynamics or lithosphere-asthenosphere interactions were involved in their maintenance or rejuvenation over long geologic time scales.

The spatial resolution of our database does not allow imaging erosion and/or deposition at the scale of the individual rifts of the Early Cretaceous rift system (Fig. 14). In other words, rift shoulders are too narrow to be mapped, although they likely formed topographic massifs and/or escarpments at the time of rifting. Nonetheless, the contribution of these rift shoulders in terms of eroded or deposited volumes is likely small compared to that of long-wavelength upwarps (Fig. 16). Indeed, rift shoulders would typically generate 1 km of tectonic relief along strips a few tens of km wide, whereas upwarps undergo hundreds of meters of denudation over 500- to 1500-km-wide areas (Fig.

16). Considering a period of 20 m.y. (typical lifetime of rift shoulder relief), a 1000-km-long and 1000-km-wide upwarp would provide 4×10^5 km³ of clastic sediments if eroded at 10 m/m.y. Total erosion of a 1-km-high, 50-km-wide rift shoulder of the same length would produce only 5×10^4 km³ of sediments. Because upwarps were eroded at ~10 m/m.y. over more than 100 m.y., the contribution of rift shoulders to the total erosion and/or deposition budget of northwestern Africa would be negligible with respect to that of its marginal upwarp(s).

Implications for Paleogeographic and Source-to-Sink Studies

Marginal upwarp segments therefore constitute long-lived source areas for clastic sediments feeding the basins. However, beyond the two Paleogene time steps (Figs. 12 and 13), the past river networks and continental divides may not be reconstructed. Nonetheless, the present work has important implications for key issues in the understanding of paired shield-passive margin source-to-sink systems. Our reconstructions indeed suggest that river systems draining the upwarp(s) fed both the intracratonic Saharan basin and the Central and equatorial Atlantic margins since at least the rifting. The source-to-sink sediment budget of marginal upwarp should therefore consider both the margin and—potentially distant—intracratonic sinks, be they marine or continental. Given that the Saharan basin was an embayment of the Tethys Ocean located north of the study area, remobilization and northward transport of intracratonic Saharan sediments have occurred. Furthermore, our reconstructions indicate that Meso-Cenozoic sediments have been tapped from the intracratonic basin and transported to the margin basins by rivers cutting across upwarp(s). This implies that intracratonic basins act as transient sediment reservoirs (i.e., sinks) that must be taken into account for source-to-sink investigations of marginal upwarps and large intracontinental sedimentary systems in general. This issue is further amplified by the late Paleogene upheaval of the Saharan basin as a consequence of hotspot swell growth (Fig. 3D), which renders actual assessment of Mesozoic intracratonic sedimentary accumulation history uncertain. Despite these complications, our study is the first to provide ways to assess the past areal extent of erosional marginal upwarps, which may be used to estimate volumetric erosional export of such upwarps using long-term denudation laws such as those calibrated by Beauvais and Chardon (2013) or Grimaud et al. (2014, 2015).

As a result of long-wavelength lithospheric deformation and coeval erosion, the current West African intracratonic basins are only residual fragments of a large Saharan basin that once covered up to two-thirds of the pre-Mesozoic continental substrate of northwestern Africa. Therefore, those basins should not be studied as separate entities. Likewise, our study shows that the Hoggar shield, which was considered by most authors as a large topographic massif since the early Mesozoic (e.g., Guiraud et al., 2005), effectively emerged only in the Late Eocene (Figs. 5–13). This emersion is the result of the bursting, distortion, and erosion of the Saharan basin by the Hoggar hotspot swell.

CONCLUSION

The construction of Meso-Cenozoic geological paleomaps allows reassessing the opening mode of the equatorial Atlantic Ocean and linking the structural, erosional, and sedimentary history of its African continental margins to that of their hinterland. Such a work has implications for the understanding of the coupling between long-wavelength deformation of a continent and sediment routing processes over paired shield continental margin systems.

Oblique rifting of the equatorial Atlantic domain started in the Valanginian (140–133 Ma), following plate reorganization and abandonment of a western rift system that was propagating from the Central Atlantic Ocean into northern South America. The equatorial Atlantic rift system propagated eastward as an en echelon pattern of alternating dextral strike-slip and normal faults until the Aptian (ca. 113 Ma). The rift system was connected to an inland rift network under an overall regime of NE-SW extension in present-day coordinates. The whole rift-transform system fragmented northwestern Africa into six microplates, and we propose a new synrift kinematic model refining the pre-opening rift of Africa and North America.

The geological reconstructions reveal the persistent or renewed occurrence of eroding upwarps along the African continental margins that provided sediments both for the margin basins and for a very large, persistent intracratonic basin. But as an embayment of the Tethys Sea, such a basin acted as a transient sediment reservoir because the products of its erosion were transferred both to the Tethys (by north-flowing rivers) and the equatorial Atlantic Ocean (by rivers crossing the marginal upwarp[s]). The source-to-sink investigation of the paired shield-continental margin system is further complicated by late Paleogene upheaval of the intracratonic basin as a result of the growth of a hotspot swells that led to the distortion and further erosion of its Meso-Cenozoic sediments. Upheaval resulted in the fragmentation of the intracratonic basin into smaller residual basins, whose pre-hotspot evolution should not be considered separately from one another. Hotspot-swell growth triggered a major reorganization of both the continental area and its margins in the Early Oligocene as has the northwestern African source-to-sink system.

ACKNOWLEDGMENTS

This study was funded by Total Exploration and Production through the Transform Source-to-Sink Project (TS2P). We acknowledge Total for providing data and for allowing publication of the study. Total R&D research group is thanked for discussions as well as scientific and technical support. We are grateful to Maryline Moulin and Daniel Aslanian for providing us with their kinematic model of the equatorial Atlantic Ocean. The paper benefited from the constructive comments of two anonymous reviewers.

REFERENCES CITED

Agyingi, C.M., 1993, Palynological evidence for a Late Cretaceous age for the Patti Formation, eastern Bida Basin, Nigeria: *Journal of African Earth Sciences*, v. 17, p. 513–523, doi:10.1016/0899-5362(93)90008-E.

Ait-Hamou, F., 2006, Le volcanisme cénozoïque à l'échelle du bombement de l'Ahaggar (Sahara Central Algerien); synthèse géochronologique et répartition spatio-temporelle quelques im-

plications en relation avec l'histoire eo-Alpine de la plaque Afrique: *Mémoires du Service géologique de l'Algérie*, v. 13, p. 155–167.

Ait-Hamou, F., and Dautria, J.M., 1994, Le magmatisme cénozoïque du Hoggar: Une synthèse des données disponibles. Mise au point sur l'hypothèse d'un point chaud: *Bulletin du Service géologique de l'Algérie*, v. 5, p. 49–68.

Akande, S.O., Ojo, O.J., Erdtmann, B.D., and Hetenyi, M., 2005, Paleoenvironments, organic petrology and Rock-Eval studies on source rock facies of the lower Maastrichtian Patti Formation, southern Bida Basin, Nigeria: *Journal of African Earth Sciences*, v. 41, p. 394–406, doi:10.1016/j.jafrearsci.2005.07.006.

Alidou, S., and Lang, J., 1983, Etude sédimentologique, paléogéographique et stratigraphique du bassin intracratonique paléozoïque-mésozoïque de Kandi (Nord-Est Bénin—Afrique de l'Ouest): *Geologische Rundschau*, v. 72, p. 191–205, doi:10.1007/BF01765906.

Alidou, S., Lang, J.L., Bonvallot, J., Roman, E., and Seilacher, A., 1991, Marine influences in the so-called continental sediments of the Paleozoic–Mesozoic Kandi Basin (northern Benin; West Africa): *Journal of African Earth Sciences*, v. 12, p. 55–65, doi:10.1016/0899-5362(91)90057-6.

Allix, P., 1983, Environnements mésozoïques de la partie nord-orientale du fossé de la Bénoué (Nigeria): *Stratigraphie-sédimentologie-evolution géodynamique*: Marseille, France, *Travaux des Laboratoires des Sciences de la Terre, Saint Jérôme, Série B*, v. 21, 200 p.

Allix, P., and Popoff, M., 1983, Le crétacé inférieur de la partie nord orientale du fossé de la Bénoué (Nigeria) un exemple de relation étroite entre tectonique et sédimentation: *Bulletin des Centres de Recherches Exploration-Production Elf-Aquitaine*, v. 7, p. 349–359.

Allix, P., Grosdidier, E., Jardine, S., Legoux, O., and Popoff, M., 1981, Découverte d'Aptien supérieur à Albien inférieur daté par microfossiles dans la série détritico crétacée du fossé de la Bénoué (Nigeria): *Comptes Rendus des Séances de l'Académie des Sciences, Série II*, v. 292, p. 1291–1294.

Allix, P., Legoux, O., and Robert, P., 1984, Essai d'interprétation géodynamique de l'évolution mésozoïque de sous-bassins du Fossé de la Bénoué (Nigeria): *Bulletin de la Société Géologique de France*, v. 26, p. 1061–1068, doi:10.2113/gssgfbull.S7-XXVI.6.1061.

Assine, M.L., 2007, Bacia do Araripe: *Boletim de Geociencias da Petrobras*, v. 15, p. 371–389.

Ault, A.K., Flowers, R.M., and Bowring, S.A., 2015, Synchronicity of cratonic burial phases and gaps in the kimberlite record: Episodic magmatism or preservational bias?: *Earth and Planetary Science Letters*, v. 410, p. 97–104, doi:10.1016/j.epsl.2014.11.017.

Avbovbo, A.A., Ayoola, E.O., and Osahon, G.A., 1986, Depositional and structural styles in Chad Basin of northeastern Nigeria: *American Association of Petroleum Geologists Bulletin*, v. 70, p. 1787–1798.

Baby, G., 2012, Analyse sédimentaire du bassin Mauritanien-Sénégalais/bassin du Cap Vert: Mise en évidence de mouvements verticaux et reconstitution de l'évolution de la marge nord-ouest africaine (Mésozoïque-Cénozoïque) [Ph.D. thesis]: Université Paul Sabatier, France, 40 p.

Baby, G., Caillaud, A., Calves, G., Guillocheau, F., Robin, C., and Leparmentier, F., 2014, Vertical movements in NW Africa margin: Controls on accommodation and sedimentary partitioning: *Geophysical Research Abstracts*, v. 16, p. 5318.

Basile, C., 2015, Transform continental margins; Part 1, Concepts and models: *Tectonophysics*, v. 661, p. 1–10, doi:10.1016/j.tecto.2015.08.034.

Basile, C., Masclé, J., and Guiraud, R., 2005, Phanerozoic geological evolution of the equatorial Atlantic domain: *Journal of African Earth Sciences*, v. 43, p. 275–282, doi:10.1016/j.jafrearsci.2005.07.011.

Basile, C., Maillard, A., Patriat, M., Gaullier, V., Loncke, L., Roest, W., Mercier de Lépinay, M., and Pattier, F., 2013, Structure and evolution of the Demerara Plateau, offshore French Guiana: Rifting, tectonic inversion and post-rift tilting at transform-divergent margins intersection: *Tectonophysics*, v. 591, p. 16–29, doi:10.1016/j.tecto.2012.01.010.

Beauvais, A., and Chardon, D., 2013, Modes, tempo, and spatial variability of Cenozoic cratonic denudation: The West African example: *Geochemistry, Geophysics, Geosystems*, v. 14, p. 1590–1608, doi:10.1002/ggge.20093.

Beauvais, A., Ruffet, G., Henocque, O., and Colin, F., 2008, Chemical and physical erosion rhythms of the West African Cenozoic morphogenesis: The ⁴⁰Ar/³⁹Ar dating of supergene K-Mn oxides: *Journal of Geophysical Research*, v. 113, F04007, doi:10.1029/2008JF000996.

Bellion, Y., Benkheilil, J., and Guiraud, R., 1984, Mise en évidence de déformations d'origine compressive dans le continental intercalaire de la partie méridionale du bassin de Taoudenni (Hodh oriental, confins mauritano-maliens): *Bulletin de la Société Géologique de France*, v. 6, p. 1137–1147, doi:10.2113/gssgfbull.S7-XXVI.6.1137.

- Benkheilil, J., 1982, Benue Trough and Benue Chain: *Geological Magazine*, v. 119, p. 155–168, doi:10.1017/S001675680002584X.
- Benkheilil, J., 1987, Cretaceous deformation, magmatism, and metamorphism in the Lower Benue Trough, Nigeria: *Geological Journal*, v. 22, p. 467–493, doi:10.1002/gj.3350220629.
- Benkheilil, J., 1988, Structure et évolution géodynamique du bassin intracontinental de la Bénoué (Nigeria): *Bulletin des Centres de Recherches Exploration-Production Elf-Aquitaine*, v. 12, p. 29–128.
- Benkheilil, J., 1989, The origin and evolution of the Cretaceous Benue Trough (Nigeria): *Journal of African Earth Sciences*, v. 8, p. 251–282, doi:10.1016/S0889-5362(89)80028-4.
- Benkheilil, J., and Guiraud, R., 1980, La Benoue (Nigeria); une chaîne intracontinentale de style atlasique: *Comptes Rendus de l'Académie des Sciences*, v. 290, p. 1517–1520.
- Benkheilil, J., Dainelli, P., Ponsard, J.F., Popoff, M., and Saugy, L., 1988, The Benue Trough; wrench-fault related basin on the border of the equatorial Atlantic, in Manspeizer, W., ed., *Triassic–Jurassic Rifting: Developments in Geotectonics*: Amsterdam, Elsevier, v. 22, p. 787–820, doi:10.1016/B978-0-444-42903-2.50037-3.
- Benkheilil, J., Mascle, J., and Tricart, P., 1995, The Guinea continental margin: An example of a structurally complex transform margin: *Tectonophysics*, v. 248, p. 117–137, doi:10.1016/0040-1951(94)00246-6.
- Benkheilil, J., Mascle, J., and Guiraud, M., 1998, Sedimentary and structural characteristics of the Cretaceous along the Cote d'Ivoire–Ghana transform margin and in the Benue Trough: A comparison, in Mascle, J., Lohmann, G.P., and Moulade, M., eds., *Proceedings of the Ocean Drilling Program: College Station, Texas, Ocean Drilling Program, Scientific Results*, v. 159, p. 93–99.
- Bennett, K.C., and Rusk, D., 2002, Regional 2D seismic interpretation and exploration potential of offshore deepwater Sierra Leone and Liberia, West Africa: *The Leading Edge*, v. 21, p. 1118–1124, doi:10.1190/1.1523743.
- Bigot-Cormier, F., Basile, C., Poupeau, G., Bouillin, J.-P., and Labrin, E., 2005, Denudation of the Côte d'Ivoire–Ghana transform continental margin from apatite fission tracks: *Terra Nova*, v. 17, p. 189–195, doi:10.1111/j.1365-3121.2005.00605.x.
- Binks, R.M., and Fairhead, J.D., 1992, A plate tectonic setting for Mesozoic rifts of West and Central Africa: *Tectonophysics*, v. 213, p. 141–151, doi:10.1016/0040-1951(92)90255-5.
- Bouillin, J.-P., Poupeau, G., Labrin, E., Basile, C., Sabil, N., Mascle, J., Mascle, G., Gillot, F., and Riou, L., 1997, Fission track study: Heating and denudation of marginal ridge of the Ivory Coast–Ghana transform margin: *Geo-Marine Letters*, v. 17, p. 55–61, doi:10.1007/PL00007208.
- Bouillin, J.P., Poupeau, G., Basile, C., Labrin, E., and Mascle, J., 1998, Thermal constraints on the Cote d'Ivoire–Ghana transform margin: Evidence from apatite fission tracks: *Proceedings of the Ocean Drilling Program, Scientific Results*, v. 159, p. 43–48.
- Bouysse, P., 2014, *Geological Map of the World*: Paris, France, Commission de la carte géologique du monde–Commission for the Geological Map of the World (CCGM-CGMW), scale 1:35,000,000.
- Brownfield, M.E., and Charpentier, R.R., 2003, Assessment of the undiscovered oil and gas of the Senegal Province, Mauritania, Senegal, the Gambia, and Guinea-Bissau, Northwest Africa: *U.S. Geological Survey Bulletin 2207-A*, 26 p.
- Brownfield, M.E., and Charpentier, R.R., 2006, Geology and total petroleum systems of the Gulf of Guinea Province of West Africa: *U.S. Geological Survey Bulletin 2207-C*, 32 p.
- Burke, K., 1976, The Chad Basin: An active intra-continental basin: *Tectonophysics*, v. 36, p. 197–206, doi:10.1016/0040-1951(76)90016-0.
- Burke, K., 1996, The African Plate: *South African Journal of Geology*, v. 99, p. 339–409.
- Burke, K., and Whiteman, A.J., 1973, Uplift, rifting and the break-up of Africa, in Tarling, D.H., and Runcorn, S.K., eds., *Implications of Continental Drift to the Earth Sciences*: London and New York, Academic Press, p. 735–755.
- Burke, K., Macgregor, D.S., and Cameron, N.R., 2003, Africa's petroleum systems: Four tectonic "Aces" in the past 600 million years, in Arthur, T.J., Macgregor, D.S., and Cameron, N.R., eds., *Petroleum Geology of Africa: New Themes and Developing Technologies*: Geological Society of London Special Publication 207, p. 21–60, doi:10.1144/GSL.SP.2003.207.3.
- Busson, G., 1971, *Principes, méthodes et résultats d'une étude stratigraphique du Mésozoïque saharien* [Ph.D. thesis]: Université Pierre et Marie Curie, France, 441 p.
- Busson, G., and Cornée, A., 1991, The Sahara from the Middle Jurassic to the Middle Cretaceous: Data on environments and climates based on outcrops in the Algerian Sahara: *Journal of African Earth Sciences (and the Middle East)*, v. 12, no. 1–2, p. 85–105, doi:10.1016/0889-5362(91)90060-C.
- Cavellec, S., 2006, Evolution diagénétique du bassin de Tim Mersoï et conséquences pour la genèse des minéralisations uranifères dans les formations carbonifères du Guezouman et du Tarat (district Arlit-Akokan, Niger) [Ph.D. thesis]: Orsay, France, Université Paris XI, 449 p.
- Chaboureau, A.C., 2012, Impact du climat et de la tectonique sur la dynamique des systèmes sédimentaires pendant l'ouverture de l'Atlantique Sud [Ph.D. thesis]: Université de Rennes 1, France, 260 p.
- Chaboureau, A.C., Guillocheau, F., Robin, C., Rohais, S., Moulin, M., and Aslanian, D., 2013, Paleogeographic evolution of the central segment of the South Atlantic during Early Cretaceous times: Paleotopographic and geodynamic implications: *Tectonophysics*, v. 604, p. 191–223, doi:10.1016/j.tecto.2012.08.025.
- Chardon, D., Grimaud, J.L., Rouby, D., Beauvais, A., and Christophoul, F., 2016, Stabilization of large drainage basins over geological time scales: Cenozoic West Africa, hot spot swell growth, and the Niger River: *Geochemistry, Geophysics, Geosystems*, v. 17, p. 1164–1181, doi:10.1002/2015GC006169.
- Chierici, M.A., 1996, Stratigraphy, palaeoenvironments and geological evolution of the Ivory Coast-Ghana basin, in *Géologie de l'Afrique et de l'Atlantique Sud: Actes Colloques Angers 1994*, p. 293–303.
- Choubert, G., and Faure-Muret, A., 1988, *International Geological Map of Africa (third edition): Commission for the Geological Map of the World (CCGM)/UNESCO, scale 1:5,000,000.*
- Clift, P.D., Lorenzo, J., Carter, A., and Hurford, A.J., 1997, Transform tectonics and thermal rejuvenation on the Cote d'Ivoire–Ghana margin, West Africa: *Journal of the Geological Society of London*, v. 154, p. 483–489, doi:10.1144/gsjgs.154.3.0483.
- Clift, P.D., Carter, A., and Hurford, A.J., 1998, Apatite fission-track analysis of sites 959 and 960 on the transform continental margin of Ghana, West Africa: *Proceedings of the Ocean Drilling Program, Scientific Results*, v. 159, p. 35–41.
- Conde, V.C., Lana, C.C., Pessoa Neto, O.C., Roesser, E.H., de Moraes Neto, J., and Dutra, D.C., 2007, Bacia do Ceara: *Boletim de Geociencias da Petrobras*, v. 15, p. 347–355.
- Cornet, A., 1943, La transgression crétacée-éocène à l'Ouest de l'Adrar des Iforas et les dépôts continentaux post-éocènes: *Travaux de l'Institut de Recherches Sahariennes (Alger)*, v. 2, p. 177–197.
- Costa, J.B.S., Bemerguy, R.L., Hasui, Y., and Borges, M. da S., 2001, Tectonics and paleogeography along the Amazon River: *Journal of South American Earth Sciences*, v. 14, p. 335–347, doi:10.1016/S0895-9811(01)00025-6.
- Cunha, P.R.C., Goncalves de Melo, J.H., and Braga da Silva, O., 2007, Bacia do Amazonas: *Boletim de Geociencias da Petrobras*, v. 15, p. 227–251.
- Da Costa, P.Y.D., Johnson, A.K.C., and Affaton, P., 2009, Biostratigraphy and geodynamic impact in the uppermost part of the northeastern coastal basin of Togo: *Comptes Rendus Palévol*, v. 8, no. 6, p. 511–526, doi:10.1016/j.crpv.2009.05.003.
- Dars, R., 1957, Sur l'existence du Continental Intercaire au NE de Nara (AOF): *Compte Rendu Sommaire des Séances de la Société Géologique de France*, p. 248–249.
- Dars, R., 1960, Les formations sédimentaires et les dolérites du Soudan occidental (Afrique de l'Ouest) [Ph.D. thesis]: Université de Paris, France, 386 p.
- Davidson, L., Beswetherick, S., Craig, J., Eales, M., Fisher, A., Himmali, A., Jho, J., Mejrab, B., and Smart, J., 2000, The structure, stratigraphy and petroleum geology of the Murzuq Basin, Southwest Libya, in Sola, M.A., ed., *Geological Exploration in Murzuq Basin, Netherlands: Amsterdam, Netherlands, Elsevier*, p. 295–320, doi:10.1016/B978-0-444-50611-5/50016-7.
- Davison, I., 2005, Central Atlantic margin basins of North West Africa: Geology and hydrocarbon potential (Morocco to Guinea): *Journal of African Earth Sciences*, v. 43, p. 254–274, doi:10.1016/j.jafrearsci.2005.07.018.
- de Almeida, F.F.M., Hasui, Y., De Brito Neves, B.B., and Fuck, R.A., 1981, Brazilian structural provinces: An introduction: *Earth-Science Reviews*, v. 17, p. 1–29, doi:10.1016/0012-8252(81)90003-9.
- Delteil, J.-R., Valery, P., Montadert, L., Fondeur, C., Patriat, P., and Mascle, J., 1974, Continental margin in the northern part of the Gulf of Guinea, in Burk, C. and Drake, C.L., eds., *The Geology of Continental Margins*: New York, Springer-Verlag, p. 297–311, doi:10.1007/978-3-662-01141-6_22.
- de Matos, R.M.D., 1992, The northeast Brazilian rift system: *Tectonics*, v. 11, p. 766–791, doi:10.1029/91TC03092.
- De Moraes Neto, J.M., Hegarty, K., and Karner, G.D., 2006, Abordagem preliminar sobre paleo-temperatura e evolucao do relevo da bacia do Araripe, nordeste do Brasil, a partir da analise de tracos de fissao em apatita: *Boletim de Geociencias da Petrobras*, v. 14, p. 113–118.

- De Moraes Neto, J.M., Green, F.P., Karner, G.D., and Flecha de Alkmim, F., 2008, Age of the Serra do Martins Formation, Borborema Plateau, northeastern Brazil; constraints from apatite and zircon fission-track analysis: *Boletim de Geociencias da Petrobras*, v. 16, p. 23–52.
- Dillon, W.P., Schlee, J.S., and Klitgord, K.D., 1988, The development of the continental margin of eastern North America—Conjugate continental margin to West Africa: *Journal of African Earth Sciences*, v. 7, p. 361–367, doi:10.1016/0899-5362(88)90080-2.
- Dufaure, P., Fourcade, E., and Massa, D., 1984, Réalité des communications marines transsahariennes entre la Téthys et l'Atlantique durant le Crétacé supérieur: *Comptes-Rendus de l'Académie des Sciences*, v. 298, no. II, p. 665–670.
- Dumestre, M.A., and Carvalho, F.F., 1985, The petroleum geology of the Republic of Guinea Bissau: *Oil & Gas Journal*, v. 83, p. 180–191.
- Ehlers, T.A., and Farley, K.A., 2003, Apatite (U-Th)/He thermochronometry: Methods and applications to problems in tectonic and surface processes: *Earth and Planetary Science Letters*, v. 206, p. 1–14, doi:10.1016/S0012-821X(02)01069-5.
- Emery, K.O., Uchupi, E., Phillips, J., Bowin, C.O., and Mascle, J., 1975, Continental margin off western Africa; Angola to Sierra Leone: *American Association of Petroleum Geologists Bulletin*, v. 59, p. 2209–2265.
- English, K.L., Redfern, J., Bertotti, G., English, J.M., and Yahia Cherif, R., 2016, Intraplate uplift: New constraints on the Hoggar dome from the Illizi basin (Algeria): *Basin Research*, doi:10.1111/bre.12182.
- Fabre, J., 2005, Géologie du Sahara occidental et central: *Tervuren African Geoscience Collection*, Tervuren, Belgium, v. 108, 572 p.
- Fabre, J., Arnaud-Vanneau, A., Belhadji, Z., and Monod, T., 1996, Evolution des terrains méso-cénozoïques d'une marge à l'autre du craton ouest africain, entre le Tanezrouft (Algérie) et l'Adrar de Mauritanie: *Mémoires du Service Géologique de l'Algérie*, v. 8, p. 187–229.
- Fairhead, J.D., 1988, Mesozoic plate tectonic reconstructions of the central South Atlantic Ocean: The role of the West and Central African rift system: *Tectonophysics*, v. 155, p. 181–191, doi:10.1016/0040-1951(88)90265-X.
- Figueiredo, J.J.P., Zalan, P.V., and Soares, E.F., 2007, Bacia da Foz do Amazonas: *Boletim de Geociencias da Petrobras*, v. 15, p. 299–309.
- Frizon de Lamotte, D., Fourdan, B., Leleu, S., Leparmentier, F., and de Clarens, P., 2015, Style of rifting and the stages of Pangea breakup: *Tectonics*, v. 34, p. 1009–1029, doi:10.1002/2014TC003760.
- Gallagher, K., Hawkesworth, C.J., and Mantovani, M.S.M., 1995, Denudation, fission track analysis and the long-term evolution of passive margin topography: Application to the southeast Brazilian margin: *Journal of South American Earth Sciences*, v. 8, p. 65–77, doi:10.1016/0895-9811(94)00042-Z.
- Gallagher, K., Brown, R., and Johnson, C., 1998, Fission track analysis and its applications to geological problems: *Annual Review of Earth and Planetary Sciences*, v. 26, p. 519–572, doi:10.1146/annurev.earth.26.1.519.
- Genik, G.J., 1992, Regional framework, structural and petroleum aspects of rift basins in Niger, Chad and the Central African Republic (CAR): *Tectonophysics*, v. 213, p. 169–185, doi:10.1016/0040-1951(92)90257-7.
- Genik, G.J., 1993, Petroleum geology of Cretaceous–Tertiary rift basins in Niger, Chad, and Central African Republic: *American Association of Petroleum Geologists Bulletin*, v. 77, p. 1405–1434.
- Gilchrist, A.R., and Summerfield, M.A., 1990, Differential denudation and flexural isostasy in formation of rifted-margin upwarps: *Nature*, v. 346, p. 739–742, doi:10.1038/346739a0.
- Gouyet, S., 1988, Evolution tectono-sédimentaire des marges guyanaise et nord-brésillienne au cours de l'ouverture de l'Atlantique Sud [Ph.D. thesis]: Université de Pau et des Pays de l'Adour, France, 374 p.
- Greigert, J., 1966, Description des formations crétaées et tertiaires du bassin des lullemedden (Afrique occidentale): Paris, France, Editions du Bureau de recherches géologiques et minières (BRGM), 236 p.
- Greigert, J., and Pougnet, R., 1967, Essai de description des formations géologiques de la République du Niger: Paris, Mémoires du Bureau de recherches géologiques et minières (BRGM), v. 48, 239 p.
- Grillot, L.R., Anderton, P.W., Haselton, T.M., and Dermargne, J.F., 1985, Three-dimensional seismic interpretation; Espoir Field area, offshore Ivory Coast: *American Association of Petroleum Geologists Memoirs*, v. 42, p. 326–329.
- Grimaud, J.L., 2014, Dynamique long-terme de l'érosion en contexte cratonique: l'Afrique de l'Ouest depuis l'Eocène [Ph.D. thesis]: Université Toulouse III Paul Sabatier, France, 300 p.
- Grimaud, J.L., Chardon, D., and Beauvais, A., 2014, Very long-term incision dynamics of big rivers: *Earth and Planetary Science Letters*, v. 405, p. 74–84, doi:10.1016/j.epsl.2014.08.021.
- Grimaud, J.L., Chardon, D., Metelka, V., Beauvais, A., and Bamba, O., 2015, Neogene cratonic erosion fluxes and landform evolution processes from regional regolith mapping (Burkina Faso, West Africa): *Geomorphology*, v. 241, p. 315–330, doi:10.1016/j.geomorph.2015.04.006.
- Guillocheau, F., Chelalou, R., Linol, B., Dauteuil, O., Robin, C., Mvondo, F., Callec, Y., and Colin, J.-P., 2015, Cenozoic landscape evolution in and around the Congo Basin: Constraints from sediments and planation surfaces, *in* de Wit, M.J., Guillocheau, F., de Wit, M.C.J., Maarten, J.W., Guillocheau, F., and Michiel, C.J.W., eds., *Geology and Resource Potential of the Congo Basin*: Berlin, Heidelberg, Springer Verlag, p. 271–313, doi:10.1007/978-3-642-29482-2_14.
- Guiraud, M., 1993, Late Jurassic rifting–Early Cretaceous rifting and Late Cretaceous transpressional inversion in the Upper Benue Basin (NE Nigeria): *Bulletin des Centres de Recherches Exploration-Production Elf-Aquitaine*, v. 17, p. 371–383.
- Guiraud, R., and Bosworth, W., 1997, Senonian basin inversion and rejuvenation of rifting in Africa and Arabia: Synthesis and implications to plate-scale tectonics: *Tectonophysics*, v. 282, p. 39–82, doi:10.1016/S0040-1951(97)00212-6.
- Guiraud, R., and Maurin, J.C., 1992, Early Cretaceous rifts of Western and Central Africa: An overview: *Tectonophysics*, v. 213, p. 153–168, doi:10.1016/0040-1951(92)90256-6.
- Guiraud, R., Bosworth, W., Thierry, J., and Delplanque, A., 2005, Phanerozoic geological evolution of Northern and Central Africa: An overview: *Journal of African Earth Sciences*, v. 43, p. 83–143, doi:10.1016/j.jafrearsci.2005.07.017.
- Gunnell, Y., 2003, Radiometric ages of laterites and constraints on long-term denudation rates in West Africa: *Geology*, v. 31, p. 131–134, doi:10.1130/0091-7613(2003)031<0131:RAOLAC>2.O.CO;2.
- Harman, R., Gallagher, K., Brown, R., Raza, A., and Bizzi, L., 1998, Accelerated denudation and tectonic/geomorphic reactivation of the cratons of northeastern Brazil during the Late Cretaceous: *Journal of Geophysical Research*, v. 103, p. 27,091–27,105, doi:10.1029/98JB02524.
- Heine, C., Zoethout, J., and Müller, R.D., 2013, Kinematics of the South Atlantic rift: *Solid Earth*, v. 4, p. 215–253, doi:10.5194/se-4-215-2013.
- Helm, C., 2009, Quantification des flux sédimentaires anciens à l'échelle d'un continent: le cas de l'Afrique au Méso-Cénozoïque [Ph.D. thesis]: Université Rennes 1, France, 364 p.
- Jermannaud, P., Rouby, D., Robin, C., Nalpas, T., Guillocheau, F., and Raillard, S., 2010, Plio-Pleistocene sequence stratigraphic architecture of the eastern Niger Delta: A record of eustasy and aridification of Africa: *Marine and Petroleum Geology*, v. 27, p. 810–821, doi:10.1016/j.marpetgeo.2009.12.005.
- Johnson, A.K., Rat, P., and Lang, J., 2000, Le bassin sédimentaire à phosphates du Togo (Maastrichtien-Eocène); stratigraphie, environnements et évolution: *Journal of African Earth Sciences*, v. 30, p. 183–200, doi:10.1016/S0899-5362(00)00015-4.
- Jourdan, F., Marzoli, A., Bertrand, H., Cirilli, S., Tanner, L.H., Kontak, D.J., McHone, G., Renne, P.R., and Bellieni, G., 2009, ⁴⁰Ar/³⁹Ar ages of CAMP in North America: Implications for the Triassic–Jurassic boundary and the ⁴⁰K decay constant bias: *Lithos*, v. 110, p. 167–180.
- Kjemperud, A., Agbesinyale, W., Agdestein, T., Gustafsson, C., and Yukler, A., 1992, Tectono-stratigraphic history of the Keta Basin, Ghana with emphasis on late erosional episodes, *in* *Géologie Africaine: Colloque de Géologie de Libreville, recueil des Communications 6–8* May 1991, p. 55–69.
- Klein, E.L., and Moura, C.A.V., 2008, São Luís Craton and Gurupi Belt (Brazil): Possible links with the West African Craton and surrounding Pan-African belts: *Geological Society of London Special Publication 294*, p. 137–151, doi:10.1144/SP294.8.
- Klitzsch, E.H., 2000, The structural development of the Murzuq and Kufra basins: Significance for oil and mineral exploration, *in* Sola, M.A., ed., *Geological Exploration of the Murzuq Basin*: Amsterdam, Netherlands, Elsevier, p. 143–150, doi:10.1016/B978-0-444-50611-5/50009-X.
- Kogbe, C.A., 1980, The Trans-Saharan Seaway during the Cretaceous, *in* Salem, M.J., and Busrewil, M.T., eds., *The Geology of Libya*: London, Academic Press, p. 91–96.
- Kogbe, C.A., 1981, Cretaceous and Tertiary of the lullemedden Basin in Nigeria (West Africa): *Cretaceous Research*, v. 2, p. 129–186, doi:10.1016/0195-6671(81)90007-0.
- Kogbe, C.A., Ajakaiye, D.E., and Matheis, G., 1983, Confirmation of a rift structure along the Mid-Niger Valley, Nigeria: *Journal of African Earth Sciences*, v. 1, p. 127–131, doi:10.1016/0899-5362(83)90004-0.
- Labails, C., 2007, La marge sud-marocaine et les premières phases d'ouverture de l'océan Atlantique Central [Ph.D. thesis]: Université de Bretagne occidentale, France, 134 p.

- Labails, C., Olivet, J.L., Aslanian, D., and Roest, W.P., 2010, An alternative early opening scenario for the Central Atlantic Ocean: *Earth and Planetary Science Letters*, v. 297, p. 355–368, doi:10.1016/j.epsl.2010.06.024.
- Lang, J., Kogbe, C., Alidou, S., Alzouma, K., Dubois, D., Houessou, A., and Trichet, J., 1986, Le Sédimentaire du Tertiaire ouest-africain et le concept de Continental Terminal: *Bulletin de la Société Géologique de France*, v. 2, p. 605–622, doi:10.2113/gssgfbull.11.4.605.
- Lang, J., Kogbe, C., Alidou, S., Alzouma, K.A., Bellion, G., Dubois, D., Durand, A., Guiraud, R., Houessou, A., de Klasz, I., Romann, E., Salard-Chebouaef, M., and Trichet, J., 1990, The continental terminal in West Africa: *Journal of African Earth Sciences*, v. 10, p. 79–99, doi:10.1016/0899-5362(90)90048-J.
- Lefranc, J.P., 1983, Corrélation vers le Nord et description stratigraphique détaillée du continental intercalaire (Mésozoïque continental) de la sebkha de Timimouns, Gourara, Sahara algérien: *Comptes Rendus des Séances de l'Académie des Sciences, Série II*, v. 296, p. 193–196.
- Lefranc, J.P. and Guiraud, R., 1990, The continental intercalaire of northwestern Sahara and its equivalents in the neighbouring regions: *Journal of African Earth Sciences*, v. 10, p. 27–77, doi:10.1016/0899-5362(90)90047-1.
- Le Marechal, A., and Vincent, P.M., 1972, Le fossé crétacé du Sud-Adamaoua, Cameroun, in Dessauvage, T.F.J., and Whiteman, A.J., eds., *Proceedings of the Conference on African Geology*: Ibadan, Nigeria, Department of Geology, University of Ibadan, Nigeria, p. 229–249.
- Leprêtre, R., 2015, Evolution phanérozoïque du Craton Ouest Africain et de ses bordures Nord et Ouest [Ph.D. thesis]: Orsay, France, Université Paris Sud, 423 p.
- Leprêtre, R., Barbarand, J., Missenard, Y., Leparmentier, F., and Frizon de Lamotte, D., 2014, Vertical movements along the northern border of the West African Craton: The Reguibat Shield and adjacent basins: *Geological Magazine*, v. 151, p. 885–898, doi:10.1017/S0016756813000939.
- Leprêtre, R., Missenard, Y., Barbarand, J., Gautheron, C., Saddiqi, O., and Pinna-Jamme, R., 2015, Post-rift history of the eastern central Atlantic passive margin: Insights from the Saharan region of South Morocco: *Journal of Geophysical Research Solid Earth*, v. 120, p. 4645–4666, doi:10.1002/2014JB011549.
- Le Roy, P., and Pique, A., 2001, Triassic–Liassic western Moroccan synrift basins in relation to the central Atlantic opening: *Marine Geology*, v. 172, p. 359–381, doi:10.1016/S0025-3227(00)00130-4.
- Liégeois, J.P., Benhallou, A., Azzouni-Sekkal, A., Yahiaoui, R., and Bonin, B., 2005, The Hoggar swell and volcanism: Reactivation of the Precambrian Tuareg shield during Alpine convergence and West African Cenozoic volcanism, in Foulger, G.R., Natland, J.H., Presnall, D.C., and Anderson, D.L. eds., *Plates, Plumes, and Paradigms: Geological Society of America Special Paper 388*, p. 379–400, doi:10.1130/0-8137-2388-4.379.
- Loule, J.P., and Pospisil, L., 2013, Geophysical evidence of Cretaceous volcanics in Logone Birni Basin (northern Cameroon), Central Africa, and consequences for the West and Central African rift system: *Tectonophysics*, v. 583, p. 88–100, doi:10.1016/j.tecto.2012.10.021.
- Luger, P., 2003, Paleobiogeography of late Early Cretaceous to early Paleocene marine Ostracoda in Arabia and north to Equatorial Africa: *Palaeogeography, Palaeoclimatology, Palaeoecology*, v. 196, p. 319–342, doi:10.1016/S0031-0182(03)00462-0.
- MacGregor, D.S., Robinson, J., and Spear, G., 2003, Play fairways of the Gulf of Guinea transform margin: *Geological Society of London Special Publication 207*, p. 131–150, doi:10.1144/GSL.SP.2003.207.7.
- Marinho, M., 1985, Le plateau marginal de Guinée: Transition entre Atlantique Central et Atlantique Equatorial [Ph.D. thesis]: Paris, France, Université Pierre et Marie Curie, 970 p.
- Marinho, M., Mascle, J., and Wannesson, J., 1988, Structural framework of the southern Guinean margin (central Atlantic): *Journal of African Earth Sciences*, v. 7, p. 401–408, doi:10.1016/0899-5362(88)90085-1.
- Mascle, J., and Blarez, E., 1987, Evidence for transform margin evolution from the Ivory Coast–Ghana continental margin: *Nature*, v. 326, p. 378–381, doi:10.1038/326378a0.
- Mateer, N.J., Wycisk, P., Jacobs, L.L., Brunet, M., Luger, P., Arush, M.A., Hendriks, F., Weissbrod, T., Gvirtzman, G., Mbede, E., Dina, A., Moody, R.T.J., Weigelt, G., El-Nakhal, H.A., et al., 1992, Correlation of nonmarine Cretaceous strata of Africa and the Middle East: *Cretaceous Research*, v. 13, p. 273–318, doi:10.1016/0195-6671(92)90003-9.
- Maurin, J.C., and Guiraud, R., 1993, Basement control in the development of the Early Cretaceous West and Central African Rift System: *Tectonophysics*, v. 228, p. 81–95, doi:10.1016/0040-1951(93)90215-6.
- Mercier de Lépinay, M., 2016, Inventaire mondial des marges transformantes et évolution tectono-sédimentaire des plateaux de Demerara et de Guinée: [Ph.D. thesis]: Perpignan, France, Université de Perpignan, 335 p.
- Milesi, J.P., Frizon de Lamotte, D., De Kock, G., and Toteu, F., 2010, Tectonic Map of Africa: Paris, Commission de la carte géologique du monde/Commission for the Geological Map of the World (CCGM/CCGM), scale 1:10,000,000.
- Mizusaki, A.M.P., Thomaz-Filho, A., Milani, E.J., and De Césaro, P., 2002, Mesozoic and Cenozoic igneous activity and its tectonic control in northeastern Brazil: *Journal of South American Earth Sciences*, v. 15, p. 183–198, doi:10.1016/S0895-9811(02)0014-7.
- Moody, R.T.J., and Sutcliffe, P.J.C., 1991, The Cretaceous deposits of the Iullemeden Basin of Niger, central West Africa: *Cretaceous Research*, v. 12, p. 137–157, doi:10.1016/S0195-6671(05)80021-7.
- Moulin, M., Aslanian, D., and Unternehr, P., 2009, A new starting point for the South and Equatorial Atlantic Ocean: *Earth-Science Reviews*, v. 97, p. 59–95.
- Ngako, V., Njonfang, E., Aka, F.T., Affaton, P., and Nnange, J.M., 2006, The north-south Paleozoic to Quaternary trend of alkaline magmatism from Niger-Nigeria to Cameroon: Complex interaction between hotspots and Precambrian faults: *Journal of African Earth Sciences*, v. 45, p. 241–256, doi:10.1016/j.jafrearsci.2006.03.003.
- Ngangom, E., 1983, Etude tectonique du fossé crétacé de la Mbéré et du Djerem, Sud-Adamaoua, Cameroun: *Bulletin des Centres de Recherches Exploration-Production Elf-Aquitaine*, v. 7, p. 339–347.
- Ojo, O.J., and Akande, S.O., 2009, Sedimentology and depositional environments of the Maastriachian Patti Formation, southeastern Bida Basin, Nigeria: *Cretaceous Research*, v. 30, p. 1415–1425, doi:10.1016/j.cretres.2009.08.006.
- Ojo, S.B., and Ajakaiye, D.E., 1976, Preliminary interpretation of gravity measurements in the middle Niger Basin area, Nigeria, in Kogbe, C.A., ed., *Geology of Nigeria: Surulere, Lagos, Nigeria, Elizabethan Publication Company*, p. 295–307.
- Olsen, P.E., 1997, Stratigraphic record of the early Mesozoic breakup of Pangea in the Laurasia-Gondwana rift system: *Annual Review of Earth and Planetary Sciences*, v. 25, p. 337–401, doi:10.1146/annurev.earth.25.1.337.
- Pessoa Neto, O.C., Soares, U.M., Fernandes da Silva, J.G., Roesner, E.H., Pires Florencio, C., and Valentin de Souza, C.A., 2007, Bacia Potiguar: *Boletim de Geociências da Petrobras*, v. 15, p. 357–369.
- Petters, S.W., 1980, Biostratigraphy of Upper Cretaceous foraminifers of the Benue Trough, Nigeria: *Journal of Foraminiferal Research*, v. 10, p. 191–204, doi:10.2113/gsjfr.10.3.191.
- Petters, S.W., 1983, Littoral and anoxic facies in the Benue Trough: *Bulletin des Centres de Recherches Exploration-Production Elf-Aquitaine*, v. 7, p. 361–365.
- Popoff, M., 1988, Du Gondwana à l'atlantique sud: les connexions du fossé de la Bénoué avec les bassins du Nord-Est brésilien jusqu'à l'ouverture du golfe de Guinée au crétacé inférieur: *Journal of African Earth Sciences*, v. 7, p. 409–431, doi:10.1016/0899-5362(88)90086-3.
- Radier, H., 1959, Contribution à l'étude géologique du Soudan oriental (AOF). Le bassin crétacé et tertiaire de Gao le détroit soudanais: *Bulletin du Service de Géologie et de Prospection Minière de l'Afrique Occidentale Française*, v. 26, no. 2, p. 337–556.
- Rat, P., Lang, J., Alzouma, K., Dikouma, M., Johnson, A., Laurin, B., Mathey, B., and Pascal, A., 1991, Coastal Marine Basins as Records of Continental Paleoenvironments (Gulf of Guinea and Iullemeden Cretaceous and Tertiary Basins): *Journal of African Earth Sciences*, v. 12, no. 1–2, p. 23–30, doi:10.1016/0899-5362(91)90054-3.
- Reymont, R.A., 1980, Biogeography of the Saharan Cretaceous and Paleocene epicontinental transgressions: *Cretaceous Research*, v. 1, p. 299–327, doi:10.1016/0195-6671(80)90041-5.
- Rouby, D., Braun, J., Robin, C., Dauteuil, O., and Deschamps, F., 2013, Long-term stratigraphic evolution of Atlantic-type passive margins: A numerical approach of interactions between surface processes, flexural isostasy and 3D thermal subsidence: *Tectonophysics*, v. 604, p. 83–103, doi:10.1016/j.tecto.2013.02.003.
- Rougier, S., 2012, Interactions lithosphère-asthénosphère et mouvements verticaux: Le cas du Massif du Hoggar [Ph.D. thesis]: Orsay, Université Paris-Sud, 277 p.
- Rougier, S., Missenard, Y., Gautheron, C., Barbarand, J., Zeyen, H., Pinna, R., Liegeois, J., Bonin, B., Ouabadi, A., Derder, M., and Frizon de Lamotte, D., 2013, Eocene exhumation of the Tuareg Shield (Sahara Desert, Africa): *Geology*, v. 41, p. 615–618, doi:10.1130/G33731.1.
- Sahagian, D.L., 1993, Structural evolution of African basins: *Stratigraphic synthesis: Basin Research*, v. 5, p. 41–54, doi:10.1111/j.1365-2117.1993.tb00055.x.
- Sapin, F., Davaux, M., Dall'Asta, M., Lahmi, M., Baudot, G., and Ringenbach, J.C., 2016, Post-rift subsidence of the French Guiana hyper-oblique margin: From rift-inherited subsidence to Amazon deposition effect: *Geological Society of London Special Publication 431*, p. 125–144, doi:10.1144/SP431.11.

- Seranne, M., and Anka, Z., 2005, South Atlantic continental margins of Africa: A comparison of the tectonic vs climate interplay on the evolution of equatorial west Africa and SW Africa margins: *Journal of African Earth Sciences*, v. 43, p. 283–300, doi:10.1016/j.jafrearsci.2005.07.010.
- Seranne, M., and Nze Abeigne, C.R., 1999, Oligocene to Holocene sediment drifts and bottom currents on the slope of Gabon continental margin (west Africa): Consequences for sedimentation and southeast Atlantic upwelling: *Sedimentary Geology*, v. 128, p. 179–199, doi: 10.1016/S0037-0738(99)00069-X.
- Simon, P., and Amakou, B., 1984, La discordance oligocène et les dépôts postérieurs à la discordance dans le bassin sédimentaire ivoirien: *Bulletin de la Société Géologique de France*, v. 26, p. 1117–1125, doi:10.2113/gssgfbull.S7-XXVI.6.1117.
- Sloss, L.L., 1963, Sequences in the Cratonic Interior of North America: *Geological Society of America Bulletin*, v. 74, p. 93–114, doi:10.1130/0016-7606(1963)74[93:SITCIO]2.0.CO;2.
- Sloss, L.L., and Scherer, W., 1975, Geometry of sedimentary basins: Applications to the Devonian of North America and Europe, in Whitten, E.H.T., ed., *Quantitative Studies in the Geological Sciences: Geological Society of America Memoir 142*, p. 71–88, doi:10.1130/MEM142-p71.
- Soares, E.F., Zalan, P.V., Picanco de Figueiredo, J.J., and Trostdorf Junior, I., 2007, Bacia do Maranhão: *Boletim de Geociências da Petrobras*, v. 15, p. 321–329.
- Soares Júnior, A.V., Costa, J.B.S., and Hasui, Y., 2008, Evolução da margem atlântica equatorial do Brasil: Três fases distensivas: *Geociências*, v. 27, p. 427–437.
- Soares Júnior, A.V., Hasui, Y., Costa, J.B.S., and Machado, F.B., 2011, Evolução do rifteamento e paleogeografia da margem Atlântica Equatorial do Brasil: Triássico ao Holoceno: *Geociências*, v. 30, p. 669–692.
- Sokari, P.B., 1992, Studies on the sedimentation and tectonics of the Yola arm of the Benue Trough: Facies architecture and their tectonic significance: *Journal of Mining and Geology*, v. 28, p. 23–31.
- Stoecklin, J., 1987, Guinea moving ahead: *Oil & Gas Journal*, v. 85, p. 91–93.
- Tari, G., Molnar, J., and Ashton, P., 2003, Examples of salt tectonics from West Africa: A comparative approach, in Arthur, T., MacGregor, D.S., and Cameron, N.R., eds., *Petroleum Geology of Africa: New Themes and Developing Technologies: Geological Society of London Special Publication 207*, p. 85–104, doi:10.1144/GSL.SP.2003.207.5.
- Trostdorf Junior, I., Zalan, P.V., Figueiredo, J.J.P., and Soares, E.F., 2007, Bacia de Barreirinhas: *Boletim de Geociências da Petrobras*, v. 15, p. 331–339.
- Turner, J.P., Rosendahl, B.R., and Wilson, P.G., 2003, Structure and evolution of an obliquely sheared continental margin: Rio Muni, West Africa: *Tectonophysics*, v. 374, p. 41–55, doi:10.1016/S0040-1951(03)00325-1.
- Turner, J.P., Green, P.F., Holford, S.P., and Lawrence, S.R., 2008, Thermal history of the Rio Muni (West Africa)–NE Brazil margins during continental breakup: *Earth and Planetary Science Letters*, v. 270, p. 354–367, doi:10.1016/j.epsl.2008.04.002.
- Valeton, I., 1991, Bauxites and associated terrestrial sediments in Nigeria and their position in the bauxite belts of Africa: *Journal of African Earth Sciences*, v. 12, p. 297–310, doi:10.1016/0899-5362(91)90078-D.
- Valsardieu, C., 1971, Etude géologique et paléogéographique du Bassin de Tim Mersoï, région d'Agadès (République du Niger) [Ph.D. thesis]: Université de Nice, 518 p.
- Vaz, P.T., da Mata Rezende, N.G., Wanderley Filho, J.R., and Travassos, W.A., 2007a, Bacia do Parnaíba: *Boletim de Geociências da Petrobras*, v. 15, p. 253–263.
- Vaz, P.T., Wanderley Filho, J.R., and Bueno, G.V., 2007b, Bacia do Tacutu: *Boletim de Geociências da Petrobras*, v. 15, p. 289–297.
- Walker, J.D., Geissman, J.W., Bowring, S.A., and Babcock, L.E., 2012, The Geological Society of America Geologic Time Scale: *Geological Society of America Bulletin*, v. 125, p. 259–272, doi:10.1130/B30712.1.
- Watts, A.B., 2001, *Isostasy and Flexure of the Lithosphere*: Cambridge, New York, Melbourne, Cambridge University Press, 508 p.
- Withjack, M.O., Schlisch, P.W., and Olsen, P.E., 1998, Diachronous Rifting, Drifting, and Inversion on the Passive Margin of Central Eastern North America: An Analog for Other Passive Margins: *American Association of Petroleum Geologists Bulletin*, v. 82, p. 817–825.
- Yang, W., and Escalona, A., 2011, Tectonostratigraphic evolution of the Guyana Basin: *American Association of Petroleum Geologists Bulletin*, v. 95, p. 1339–1368, doi:10.1306/01031110106.
- Zalán, P.V., 2007, Bacias de Bragança-Viseu, São Luís e Ilha Nova: *Boletim de Geociências da Petrobras*, v. 15, p. 341–345.
- Zalán, P.V., and Matsuda, N.S., 2007, Bacia do Marajó: *Boletim de Geociências da Petrobras*, v. 15, p. 311–319.
- Zanguina, M., Bruneton, A., and Gonnard, R., 1998, An Introduction to the Petroleum Potential of Niger: *Journal of Petroleum Geology*, v. 21, p. 83–103, doi:10.1111/j.1747-5457.1998.tb00647x.